Bioorganic Chemistry 110 (2021) 104755

Contents lists available at ScienceDirect

Bioorganic Chemistry

journal homepage: www.elsevier.com/locate/bioorg

Design and synthesis of novel glycyrrhetin ureas as anti-inflammatory agents for the treatment of acute kidney injury

Hongbo Wang [a,1], Jiawei Zuo [b,c,1], Liang Zha [c], Xia Jiang [c], Caixia Wu [a], Yong-An Yang [d], Wenjian Tang [a,c,*], Tianlu Shi [b,*]

[a] Department of Pharmacy, Shandong Medical College, Linyi 276000, China
[b] First Affiliated Hospital of USTC, Division of Life Sciences and Medicine, University of Science and Technology of China, Hefei, Anhui, 230001, China
[c] School of Pharmacy, Anhui Medical University, Hefei 230032, China
[d] Elion Nature Biological Technology Co., Ltd, Nanjing 210038, China

ARTICLE INFO

Keywords:
Glycyrrhetinic acid
Urea
Amino acid
Anti-inflammatory activity
Inflammatory factor
Acute kidney injury

ABSTRACT

To develop new anti-inflammatory drugs for the prevention and treatment of acute kidney injury, a series of novel glycyrrhetic ureas were designed, synthesized and evaluated for anti-inflammatory activity using RAW264.7 cells. Compounds **5r-5u** (2.04, 2.50, 3.25 and 2.48 μM, respectively) with acidic or neutral amino acid showed potent anti-inflammatory activity (IC_{50} = 2–3 μM for NO inhibition), amongst them, compound **5r** also inhibited tumor necrosis factor-α (TNF-α) and interleukin-6 (IL-6) in a dose-dependent manner. In cisplatin-induced AKI mice model, compound **5r** significantly reduced the level of pro-inflammatory factors, ameliorated the pathological damage of kidney tissue, and maintained the normal metabolic capacity.

1. Introduction

Acute kidney injury (AKI) is a global public health problem that affects millions of patients worldwide. Approximately 20% of hospitalized patients develop this type of injury and are accompanied by volume overload, electrolyte disturbances, uremia complications, and drug toxicity [1]. As a clinical multiple syndrome, AKI is the rapid loss of renal function that is characterized by oliguria, nephritis, and renal vein thrombosis due to the abrupt decline of glomerular filtration [2–4]. In ischemia, sepsis and nephrotoxic models, the morphological and/or functional changes are observed in vascular endothelial cells and/or in tubular epithelium. Then, leukocytes including neutrophils, macrophages, natural killer cells, and lymphocytes infiltrate into the injured kidneys. The injury induces the generation of inflammatory mediators like cytokines and chemokines by tubular and endothelial cells which contribute to the recruiting of leukocytes into the kidneys. Inflammation is a reaction of the immune system, which activates many enzymes and cellular processes to protect the body from various injuries [5]. Thus, inflammation plays an important role in the initiation and extension phases of AKI [6,7]. Kidney inflammation is the initial response to kidney stress or injury, it protects the kidney from further damage [8]. Clinical manifestations have proved that AKI is associated with intrarenal and systemic inflammation, which is essential for eliminating microbial pathogens and repairing tissue after diverse forms of injury [9–11]. Continued active research in the fields of chemistry and biology has contributed to pharmaceuticals to alleviate pain and other associated damage, which is reported in 90% of cases according to World Health Organization (WHO) statistics [12]. To date, no effective chemical agents have been developed to prevent or alleviate AKI in the clinic. Therefore, it is urgent to develop novel therapies to improve renal regeneration capacity, preserve renal function and prevent AKI.

Inflammation is the basic defense mechanism of the immune system and bound up with a great range of diseases, which can prevent damage caused by harmful stimuli such as pathogens and poisons. Non-steroidal anti-inflammatory drugs (NSAIDs) are the most commonly used anti-inflammatory agents, but gastrointestinal complications such as gastric ulcer and duodenal ulcer cannot be avoided, hence, there is necessary to find new drug molecules that effectively reduce inflammation and pain relief [13,14]. Renal inflammation is not only a response to pathogens, but also to sterile stimuli such as ischemia, hyperglycemia, and lipids

* Corresponding authors at: School of Pharmacy, Anhui Medical University, Hefei 230032, China (W. Tang); First Affiliated Hospital of USTC, Division of Life Sciences and Medicine, University of Science and Technology of China, Hefei, Anhui, 230001, China (T. Shi).
E-mail addresses: ahmupharm@126.com (W. Tang), tianlu828@163.com (T. Shi).
[1] H.B. Wang and J.W. Zuo contributed equally to this work.

https://doi.org/10.1016/j.bioorg.2021.104755
Received 24 December 2020; Received in revised form 6 February 2021; Accepted 17 February 2021

[15,16]. The effective treatment was achieved by overcoming the serious AKI complications through the strategy of controlling the development of inflammation. Perindopril protected AKI caused by septic shock, FTY720 prevented kidney ischemic reperfusion injury by regulating mitochondria biogenesis in dendritic cells, omeprazole attenuated cisplatin-induced kidney injury through suppression of the TLR4/NF-κB/NLRP3 signaling pathway [17–19]. While 7-hydroxycoumarin protected cisplatin-induced AKI by inhibiting necroptosis and promoting Sox9-mediated tubular epithelial cell proliferation, a rutaecarpine derivative alleviated AKI by targeting PDE4B, which is the key enzyme mediating inflammation in cisplatin nephropathy [20,21]. Although marked drugs and natural products would help to understand the mechanism of AKI, it is significant for finding new scaffolds with high efficiency and low toxicity for the treatment of AKI.

Glycyrrhetinic acid (GA), one of the main active ingredients of Licorice, exhibited a variety of pharmacological activities such as anti-inflammatory, antioxidant, antiviral and hepatoprotective activities, etc [22–25]. Renal protective effects of GA may be relevant to its anti-inflammatory activity, and recent studies have shown that GA improves nephrotoxicity and kidney injury caused by multiple etiologies through various pathways [26–28]. Interestingly, almost half of the approved new molecular entities were derived from natural products, which play a pivotal role in the search for new anti-inflammatory drugs with improved drug properties and reduced side effects [29,30]. The semi-synthesis and synthetic synthesis of natural compounds show a variety of biological applications [31]. The structural modification of biologically active natural products according to molecular characteristics was an important way to find new lead compounds, for example, structural changes of GA can improve its efficiency and decrease its toxicity [32–37].

Minor structural changes in triterpenoids can cause extensive changes in biological activity in medicinal chemistry. The therapeutic application of amino acids has received great attention in renal failure, respiratory tract, cardiology, neurological disorders and congenital defects [38]. Most of structural modifications of GA at 3-hydroxy (or 3-oxo) or/and 30-carboxylic groups exhibited a better activity than GA [32–39]. Urea scaffold (Fig. 1) was often incorporated to modulate drug potency and selectivity and improve drug properties in drug design and medicinal chemistry due to the capability of the urea functionality to form multiple stable hydrogen bonds with protein and receptor targets [40,41]. The first soluble epoxide hydrolase (sEH) inhibitor AR9281 showed anti-inflammatory activity through the urea moiety binding to the catalytic residue of sHE, while protein–ligand complexes between vascular endothelial growth factor receptor 2 (VEGFR2) and lenvatinib highlighted the importance of the urea functionality involving critical hydrogen bonding with Asp1046 and Glu885 of VEGFR2 [42,43]. Therefore, the urea moiety could be introduced into the structure of GA, which may improve potency and drug-like properties of GA.

Fragment splicing is a primary strategy in the design and optimization of natural product toward new skeleton with target bioactivity. Herein we proceeded with modification of the GA structure using following strategies: (a) converting carboxyl acid group at C30 into a urea moiety in ring E of GA, namely glycyrrhetin urea (**5c**); (b) amino of urea modified with alkyl, cycloalkyl or amino acid functionality (Fig. 1). Thus, twenty-four compounds were designed, synthesized and evaluated for their anti-inflammatory activity in lipopolysaccharide (LPS)-induced RAW264.7 cells. Further, potent compound **5r** with acidic amino acid were used to study the preliminary mechanism of anti-inflammatory effect for the treatment of AKI in cisplatin-induced AKI mice models.

2. Results and discussion

2.1. Chemistry

The preparation of the key intermediate **3** was prepared as previously reported [33] and outlined in Scheme 1. Acylation reaction of 3-OH of glycyrrhetinic acid with acetic anhydride gave 3-acetyl-glycyrrhetinic acid (**2**). Substitution reaction of 30-carboxylic acid of compound **2** and thionyl chloride in chloroform gave 3-acetyl glycyrrhetinic 30-acyl chloride, and then which was converted to the acyl azide with NaN_3 in acetone and water. The key intermediate isocyanate **3** was obtained from 3-acetyl glycyrrhetinic 30-acyl azide by Curtius rearrangement reaction in anhydrous toluene. Glycyrrhetin urea derivatives **5** were obtained from the nucleophilic addition reaction of intermediate **3** with various substituted amines or amino acids.

Reagents and conditions: (i) Ac_2O-C_5H_5N, rt, 2 h; refluxed, 2 h; (ii) $SOCl_2$, $CHCl_3$, refluxed, 2 h: NaN_3, acetone-H_2O, 5 °C, 1 h; toluene, 75 °C, 6 h; (iii) substituted amines or amino acids, ethyl acetate and methanol, rt, 1 h; (iv) NaOH, CH_3OH, rt, 12 h.

2.2. Cytotoxicity evaluation of glycyrrhetin ureas

The effects of glycyrrhetin ureas at the same concentration (20 μM) on RAW264.7 cells were examined by MTT assay. At this concentration, the effects of glycyrrhetin ureas on cell viability was not obvious, indicating that the toxicity of synthesized compounds was low (Table 1). It can be seen from the table that the cell viability percentage of tested compounds is above 80%. Thus, all compounds at this concentration are suitable for subsequent biological evaluation.

2.3. Suppression of NO production in LPS-stimulated RAW264.7 cells

Nitric oxide (NO) plays an important role in the immune system and is involved in the pathogenesis and control of infectious diseases, tumors, chronic degenerative diseases and autoimmune processes [44]. To evaluate the anti-inflammatory effect of glycyrrhetin ureas, Griess reagent was used to detect the level of the LPS-induced NO release in the

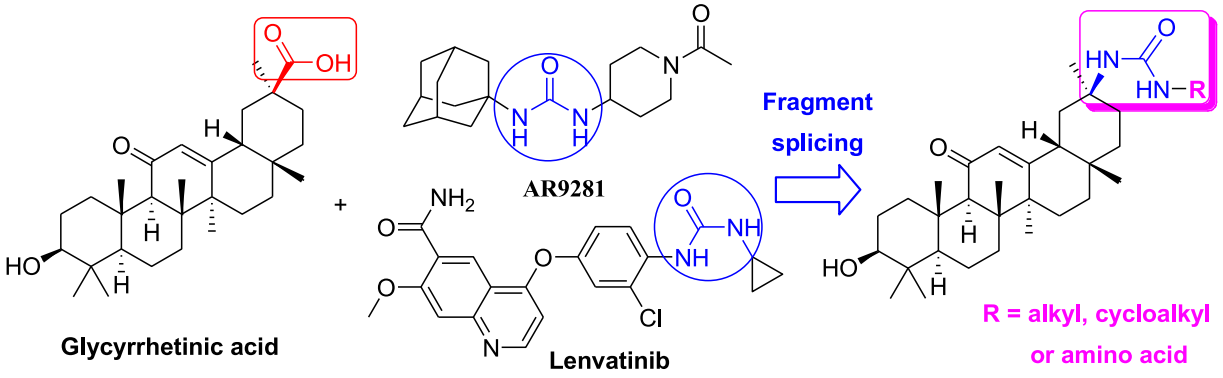

Fig. 1. The general design strategy in this study.

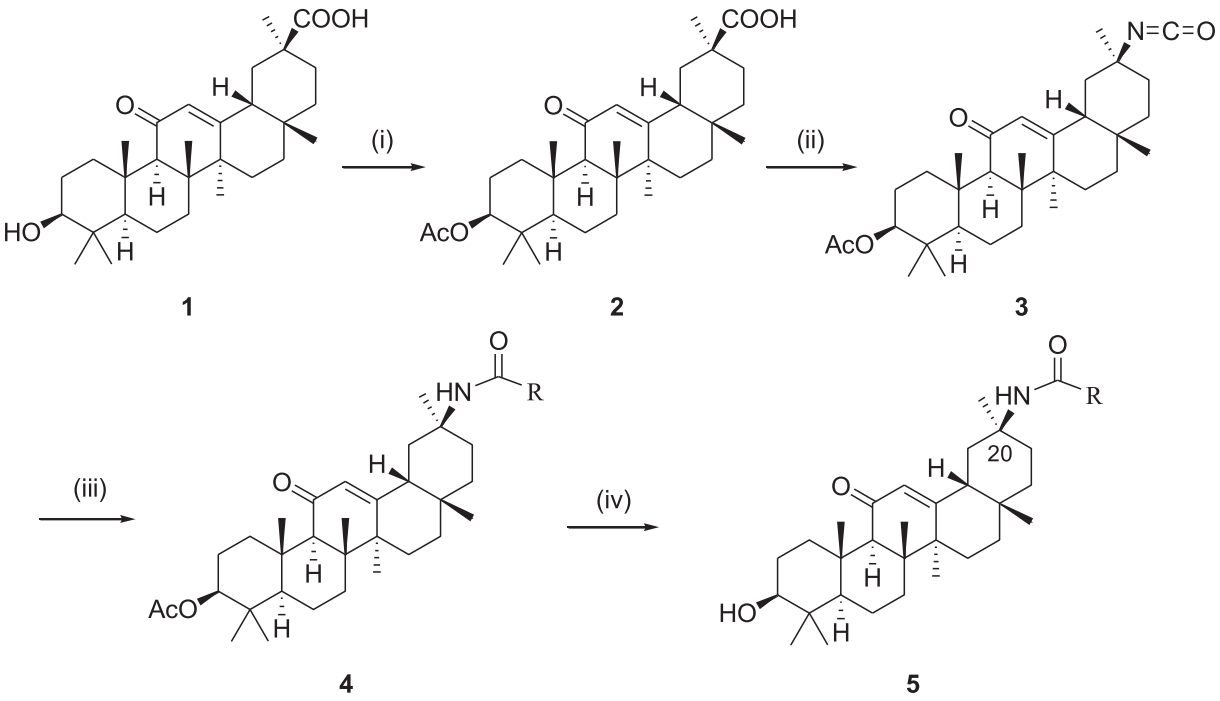

Scheme 1. Synthesis of glycyrrhetin urea derivatives **4** and **5**.

Table 1
Effect of glycyrrhetin ureas on the viability of RAW264.7 cells.

Compound	Cell viability (%) [a]	Compound	Cell viability (%) [a]
control	100	**5j**	96.8 ± 14.1
GA	85.6 ± 4.0	**5k**	87.4 ± 4.6
4a	93.4 ± 11.4	**5l**	90.7 ± 2.5
5a	86.1 ± 8.0	**5m**	89.3 ± 3.6
5b	87.3 ± 1.1	**5*n***	102.8 ± 17.5
5c	83.7 ± 13.1	**5o**	85.6 ± 4.2
4d	101.5 ± 9.0	**5p**	82.7 ± 9.4
4e	90.3 ± 10.3	**5q**	92.8 ± 5.2
5e	97.4 ± 7.4	**5r**	81.7 ± 8.6
5f	103.7 ± 2.3	**5 s**	95.3 ± 5,5
5 g	109.6 ± 13.7	**5 t**	85.8 ± 14.0
5 h	97.3 ± 11.2	**5u**	87.0 ± 8.5
5i	93.5 ± 3.1	**5v**	91.3 ± 2.1

[a] The results were showed as means ± SD of at least three independent experiments.

RAW264.7 cells. LPS treatment caused significant increase of NO release compared to blank, after pre-treatment with glycyrrhetin ureas at the concentration of 20 μM, the production of LPS-induced NO could be reduced in the supernatant. As shown in Table 2, most of glycyrrhetin ureas exhibited benign anti-inflammatory activity, amongst them, compounds **5i**, **5 k**, **5 l**, **5r**, **5 s**, **5 t** and **5u** significantly alleviated the increase of LPS-induced NO release (IC_{50} = 3.05, 3.17, 3.02, 2.04, 2.50, 3.25 and 2.48 μM, respectively). The structure–activity relationship (SAR) of NO inhibitory activity of glycyrrhetin urea was followed as bellow: (i) the NO inhibitory activity decreased when the 3-OH was acetylated (**5a** > **4a**; **5e** > **4e**); (ii) for the $\mathbf{R_2}$ position of urea unit, smaller substituent showed better NO inhibitory activity, for example, when the $\mathbf{R_2}$ substituent was the cyclamine, the activity of compound **5i** with the five-member ring is better than those of compounds **5 g**, **5 h** and **5f** with the six-member ring (IC_{50} values, μM: **5i** (cyclopentamine), 3.05 > **5 g** (cyclohexane), 16.27; **5 h** (morpholine), 17.84; **5f** (piperazine-NMe), 18.24); when the $\mathbf{R_2}$ substituent was the aliphatic amine, the activity of compounds with methyl was more potent (IC_{50} values, μM: **5 l** (-NHMe), 3.02 > **5p** (-NMe_2), 9.15 ≫ **5 m** (-NHEt), 1.3%; **5n** (-NHPr-*i*), 13.9%; **5o** (-NHBu-*n*), 19.0%); (iii) compounds **5a**, **5r**, **5 s**, **5 t** and **5u** with acidic or neutral amino acids showed significant NO inhibitory activity (IC_{50} = 14.85, 2.04, 2.50, 3.25 and 2.48 μM, respectively), while compound **5v** with basic amino acids had weak NO inhibitory activity (inhibition rate = 2.6% at 20 μM); (iv) compounds **5j** and **5 k** with 3- and 4-pyridylmethyl at the $\mathbf{R_2}$ position displayed potent anti-inflammatory activity (IC_{50} = 14.47 and 3.17 μM, respectively). Compound **5r** was the most potent for further study of the anti-inflammatory mechanism.

2.4. Compound *5r* inhibited TNF-α and IL-6 production

LPS-activated macrophages produce a variety of inflammatory cytokines, including tumor necrosis factor (TNF-α) and interleukins (IL*s*), which have a host defense effect under inflammatory conditions and maintain normal cell conditions [45]. The special plasticity of macrophages determines that it may be related to renal fibrosis and renal tissue repair, so controlling their balance is crucial. To further evaluate the effects of compound **5r** on the pro-inflammatory factors induced by LPS, in the presence of compound **5r**, RAW264.7 cells were incubated with LPS (0.5 μg/mL) for 24 h, and the TNF-α and IL-6 levels in the supernatant were determined by ELISA. As shown in Fig. 2, compared with the basal level of cytokines in macrophages in the control group, LPS stimulation significantly increased the levels of TNF-α and IL-6. After treatment with compound **5r**, the production of LPS-induced TNF-α and IL-6 was inhibited in a concentration-dependent manner (Fig. 2). These results indicated that compound **5r** reduced the excessive immune response in RAW 264.7 cells by blocking the increase of pro-inflammatory cytokines stimulated by LPS. Excessive pro-inflammatory factors such as TNF-α and IL-6 led to severe systemic diseases and high mortality [46], while compound **5r** showed fine inhibitory activity.

2.5. In vivo activity evaluation of AKI mice

2.5.1. Assessment of the Kidney/Body mass index and renal function

All mice were weighed before anesthesia, and after euthanasia, the kidneys were surgically removed and weighed. The kidney/body mass index is calculated as follows: kidney weight/body weight × 100% [47]. Compared with the blank control group, cisplatin caused kidney tissue

Table 2
The inhibitory effects of glycyrrhetic ureas on NO production in LPS-stimulated RAW 264.7 cells.

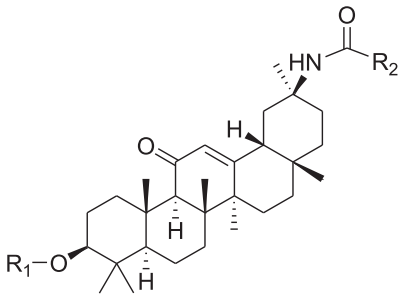

Compound	R_1	R_2	IC_{50} (μM) [a,b] or Inhibition rate % [a,b,c]
GA			12.5 ± 2.8%
4a	CH_3CO	—$NHCH_2COOH$	18.7 ± 3.1%
5a	H	—$NHCH_2COOH$	14.85 ± 1.92
5b	H	—$NHCH_2COOCH_3$	33.5 ± 2.1%
5c	H	—NH_2	*na* [d]
4d	CH_3CO	—NHOH	12.03 ± 2.70
4e	CH_3CO	—$NHCH_2CH_2OH$	*na*
5e	H	—$NHCH_2CH_2OH$	34.8 ± 3.5%
5f	H	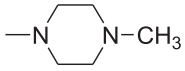	18.24 ± 1.75
5g	H	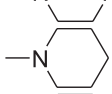	16.27 ± 3.94
5h	H	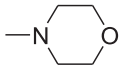	17.84 ± 2.83
5i	H		3.05 ± 0.66
5j	H	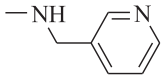	14.47 ± 3.84
5k	H	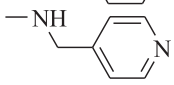	3.17 ± 1.12
5l	H	—$NHCH_3$	3.02 ± 0.92
5m	H	—$NHCH_2CH_3$	1.3 ± 0.7%
5*n*	H	—$NHCH(CH_3)_2$	13.9 ± 2.6%
5o	H	—$NH(CH_2)_3CH_3$	19.0 ± 3.1%
5p	H	—$N(CH_3)_2$	9.15 ± 1.80
5q	H	—$NH(CH_2)_2N(CH_3)_2$	13.10 ± 1.69
5r	H	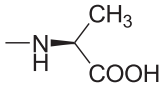	2.04 ± 1.47
5s	H	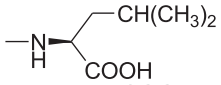	2.50 ± 1.15
5t	H	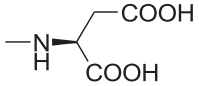	3.25 ± 0.52
5u	H	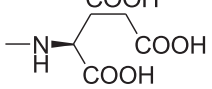	2.48 ± 1.33
5v	H	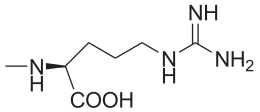	2.6 ± 1.4%

[a] The results were showed as means ± SD of at least three independent experiments.
[b] Griess reagent was detected NO production.
[c] The percentages of NO inhibition were measured at the concentration of 20 μM.
[d] *na* = no activity at the concentration of 20 μM.

injury and the kidney/body mass index increased significantly. However, compound **5r** obviously reduced the index value (Fig. 3).

Clinical data have shown that about one-third of patients develop AKI after cisplatin treatment, accompanied by decreased glomerular filtration rate, increased blood urea nitrogen (BUN) and serum creatinine (Scr), and electrolyte imbalance [48,49]. Urea and creatinine are common indicators of renal function tests, reflecting the degree of impaired glomerular filtration function and basal metabolism. As diagnostic criteria for nephrotoxicity, urea and creatinine can reflect the late manifestations of the disease, but early intervention is essential for effective treatment of AKI [50]. Serum markers of renal function were determined with BUN and Scr assay kits, according to the manufacturer's instructions. Cisplatin-treated group significantly increased Scr and BUN levels compared with normal group. Renoprotective effect of compound **5r** (30 mg/kg) was further confirmed by detecting Scr and BUN which indicated renal function (Fig. 4C and 4D).

2.5.2. *Pro-inflammatory mediators' levels in serum*

The release of TNF-α induced other inflammatory cytokines and led to an inflammatory response [51,52]. These inflammatory mediators further caused damage to renal tubular cells and renal tissues, so, the activity of compound **5r** to suppress inflammatory levels in cisplatin-induced mice was evaluated. In model group, there was marked increase of TNF-α and IL-6 after administration of cisplatin (20 mg/kg), compared with normal group (Fig. 4A and 4B). On the other hand, pretreatment and treatment with compound **5r** (30 mg/kg) antagonized cisplatin-induced elevation of TNF-α and IL-6 compared with cisplatin-treated group (Fig. 4A and 4B). Compound **5r** reduced proinflammatory response during cisplatin nephrotoxicity and the ensuing acute kidney injury and renal failure, through decreasing the levels of inflammatory mediators TNF-α and IL-6.

2.5.3. *Histopathological Analysis.*

Tubular injury is an important feature of AKI, which may eventually lead to tubulointerstitial fibrosis [53,54]. We assessed the treatment effect of compound **5r** in cisplatin nephropathy. Kidney tissue was fixed in 10% formalin and embedded in paraffin. Cut sections with a thickness of 5 μm and stain with H&E and PAS, and then take a photo with an optical microscope. On examination of kidney section, cisplatin caused necrosis of renal tubular epithelial cells and degenerative changed in the cortical and corticomedullary portions. As shown in Fig. 5, in the blank control group, the photograph clearly showed the normal shape of the glomerulus and proximal tubules. In cisplatin-induced AKI mice, renal tissues were displayed severe pathological damage, leading to tubular cell damage, inflammatory cell infiltration, and tubular dilatation. However, after treatment with compound **5r**, the nephrotoxicity caused by cisplatin in C57BL/6 mice was significantly alleviated.

3. Conclusions

Cisplatin treatment increases expression of inflammatory cytokines and chemokines in the kidney, and the inflammatory response accelerates the development of renal tissue damage and renal failure. To discovery better anti-inflammatory agents, a series of glycyrrhetic ureas **4a**, **4d**, **4e** and **5a–5v** were designed and synthesized. Most of compounds had anti-inflammatory activity, amongst them, compounds **5i**, **5 k**, **5 l**, **5r**, **5 s**, **5 t** and **5u** exhibited significant anti-inflammatory activity (IC_{50} = 3.05, 3.17, 3.02, 2.04, 2.50, 3.25 and 2.48 μM, respectively). SAR analysis showed: (i) when the 3-OH was acetylated, the NO inhibition decreased; (ii) for whether the cyclamine or the aliphatic amine at the $\mathbf{R_2}$ position, smaller substituent showed better NO inhibition; (iii) the acidic or neutral amino acid at the $\mathbf{R_2}$ position significantly increased the NO inhibition, so did the pyridylmethyl. Compound **5r** had the most potent anti-inflammatory activity and selected to further study the action mechanism. Compound **5r** also reduced the level of proinflammatory factors (TNF-α and IL-6) in a dose-dependent manner. In

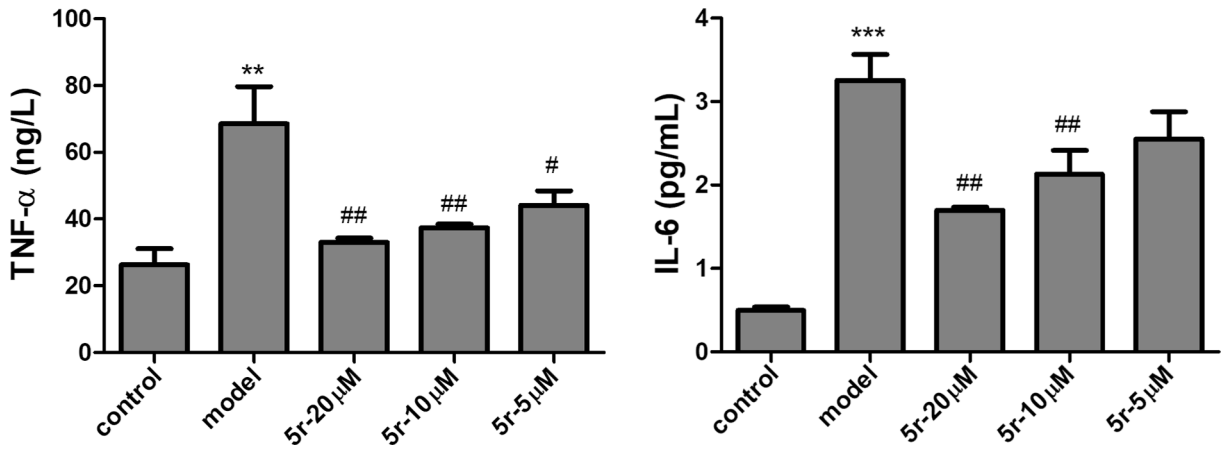

Fig. 2. Compound **5r** inhibited the cytokine production of RAW264.7 cells stimulated by LPS. RAW264.7 cells were pretreated with compound **5r** , at concentrations of 20, 10, 5 μM for 1 h, then incubated with LPS (0.5 μg/mL) for 24 h. The levels of TNF-α and IL-6 in the culture medium were measured by ELISA kits. $^{***}p <$ 0.001vs control group, $^{\#\#}p < 0.01$, $^{\#}p < 0.05$ vs model group.

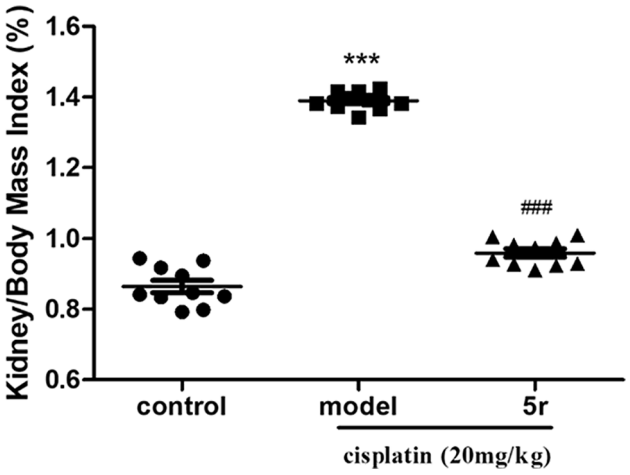

Fig. 3. The effect of compound **5r** on kidney/body mass index (%). The mice and kidney tissues of each group were weighed and recorded.

cisplatin-induced AKI mice, compound **5r** not only lowered the levels of serum pro-inflammatory factors, but also improved the renal function markers including serum creatinine and urea nitrogen. Pathologically, compound **5r** reduced inflammatory cell infiltration, relieved renal tubular cell damage and tubular dilatation.

4. Experimental section

4.1. Chemistry

All reagents were purchased from commercial sources and were used without further purification. Melting points (uncorrected) were determined on a XT4MP apparatus (Taike Corp., Beijing, China). ^{1}H NMR and ^{13}C NMR spectra were recorded on Bruker AV-500 or AV-400 MHz instruments in DMSO-d_6 or $CDCl_3$. Chemical shifts are reported in parts per million (δ) downfield from the signal of tetramethylsilane (TMS) as internal standards. Coupling constants are reported in Hz. The multiplicity is defined by *s* (singlet), *d* (doublet), *t* (triplet), or *m* (multiplet). High resolution mass spectra (HRMS) were obtained on an Agilent 1260–6221 TOF mass spectrometry. Column and thin-layer chromatography (CC and TLC, resp.) were performed on silica gel (200–300 mesh) and silica gel GF_{254} (Qingdao Marine Chemical Factory) respectively.

*4.2. The synthesis of glycyrrhetic isocyanate **3***

This compound was prepared as previously reported [33]: A solution of glycyrrhetic acid (2.5 g, 5.3 mmol) in pyridine (10 mL) and THF (20 mL) was added acetic anhydride (1.0 mL, 11 mmol) over 30 min, and the mixture was stirred and heated to reflux for 2 h. The reaction solution was evaporated *in vacuum*, and the residue was recrystallized from ethanol to obtain glycyrrhetic acid acetate **2**. (white power, 2.3 g, 85%)

Thionyl chloride (0.58 mL, 8.0 mmol) was added to a solution of **2** (1.0 g, 2.0 mmol) in $CHCl_3$ (60 mL), and the mixture was heated to reflux for 2 h. The reaction solution was evaporated *in vacuum*, and the residue triturated using diethyl ether. The precipitate was filtered and dried in vacuo to yield acyl chloride of 3-acetyl glycyrrhetinic acid, which was dissolved in acetone (200 mL).

Sodium azide (0.39 g, 6.0 mmol) in water (50 mL) was dropwise added to the solution of acyl chloride of 3-acetyl glycyrrhetinic acid at 0–5 °C over 30 min. Then the reaction mixture was stirred at 0–5 °C for 1 h and twice extracted with methylbenzene. The combined organic phase was washed three times with water, then dried over anhydrous Na_2SO_4 and filtered. The filtrates were heated to 75 °C and stirred for 6 h at the same temperature. The reaction solution was evaporated *in vacuum*, and the residue was recrystallized from EtOAc to obtain isocyanate **3**. White powder, 67%; ^{13}C NMR (100 MHz, $CDCl_3$) δ 200.0 (C-11), 171.2 (CH_3CO), 168.4 (C-13), 128.8 (C-12), 122.3 (NCO), 80.8 (C-3), 61.9 (C-9), 58.8 (C-20), 55.2 (C-5), 47.4 (C-18), 45.6 (C-19), 44.7 (C-14), 43.4 (C-8), 39.0 (C-4), 38.2 (C-1), 37.2 (C-10), 36.4 (C-16), 35.0 (C-17), 32.9 (C-7), 32.1 (C-22), 32.0 (C-29), 28.4 (C-23), 28.2 (C-28), 26.5 (C-21), 26.4 (C-2), 23.7 (C-15), 23.5 (C-27), 21.5 (CH_3CO), 18.9 (C-25), 17.6 (C-6), 16.9 (C-24), 16.6 (C-26).

*4.3. General procedures for converting the glycyrrhetic isocyanate to urea for compounds **4** and **5**.*

Method **A**: To the solution of the isocyanate **3** (1.0 mmol) in EtOAc (60 mL), the substituted amine (1.2 mmol) was added and the reaction mixture was stirred at room temperature. After 2 h, water (50 mL) was added to the reaction mixture and the organic phase was separated. The aqueous layer was twice extracted with EtOAc (2 × 30 mL). The combined organic phase was washed twice with water (2 × 30 mL), dried over anhydrous Na_2SO_4, filtered and concentrated under the reduced pressure. The residue **4** was added methanol (30 mL) and NaOH (20 mmol), and the reaction mixture was stirred at room temperature for 12 h. Water (50 mL) was added and the pH was adjusted to 3 using diluted HCl. The reaction mixture was twice extracted with EtOAc (2 × 60 mL). The combined organic phase was washed twice with water (2 × 30 mL),

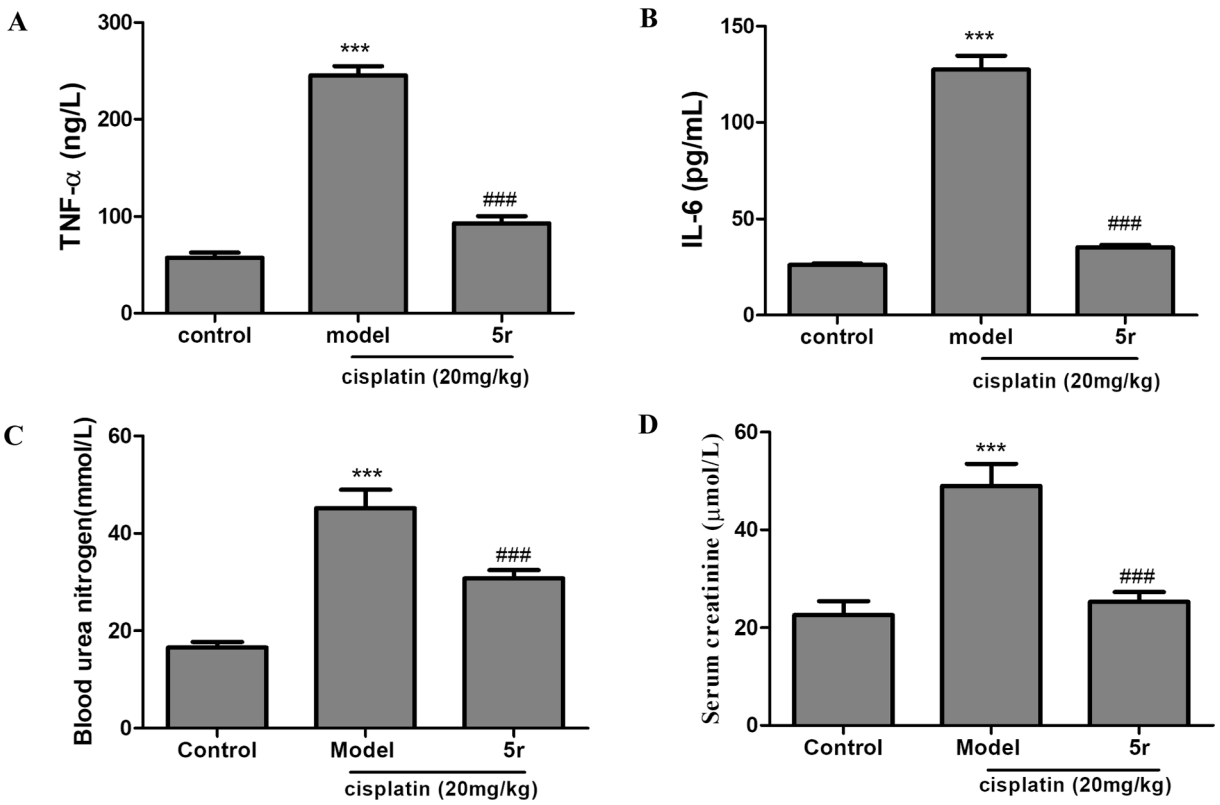

Fig. 4. The effect of compound **5r** on cisplatin-induced AKI mice. After pre-treatment with compound **5r** (30 mg/kg), the mice were injected intraperitoneally with cisplatin (20 mg/kg) and sacrificed 72 h later. Detection of kidney function markers (BUN and Scr) and pro-inflammatory factors (TNF-α and IL-6) levels in serum. $^{***}p < 0.001$ compared with control group; $^{\#\#\#}p < 0.001$ compared with model group.

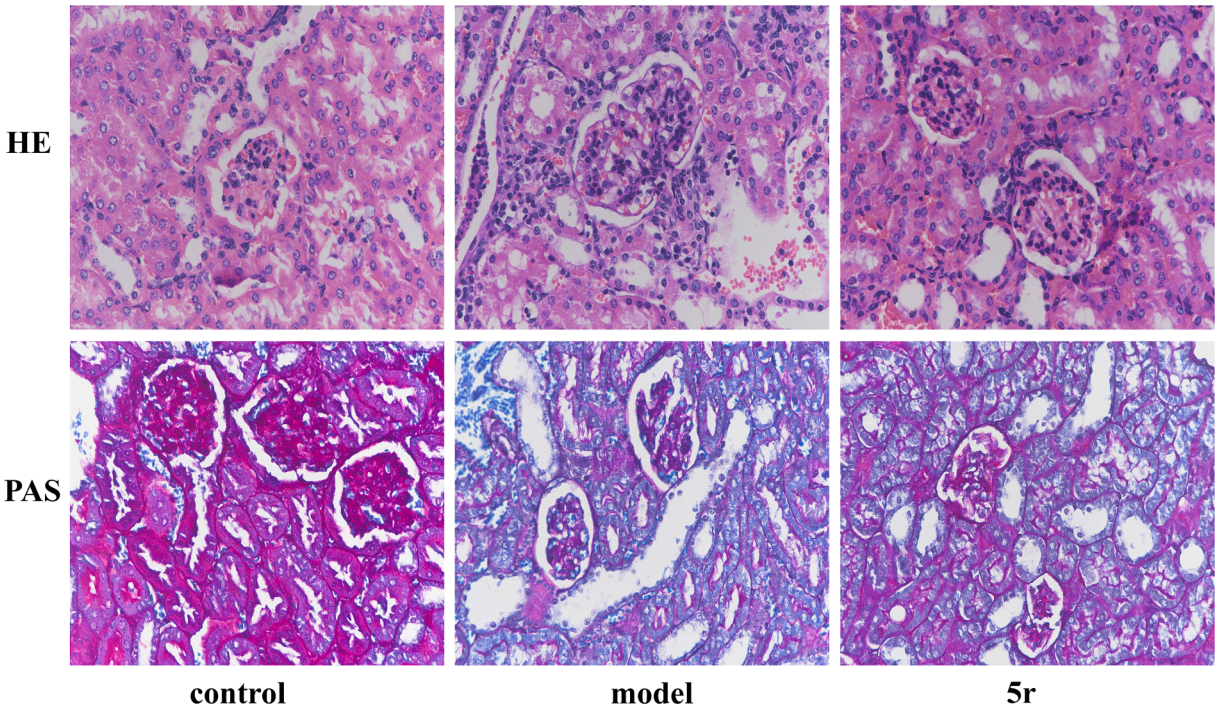

Fig. 5. Effect of compound **5r** on cisplatin-induced AKI in C57BL/6 mice. Kidney tissue was stained by H&E and PAS for histological examination.

dried over anhydrous Na_2SO_4, filtered and concentrated under the reduced pressure. The residue was purified by flash chromatography (SiO_2, MeOH-CH_2Cl_2, gradient elution) to give the urea product **5**.

Method **B**: The solution of the substituted amine hydrochloride or amino acid (1.2 mmol) in water (30 mL) and methanol (30 mL) was alkalified with diluted NaOH to pH 11–12. The solution of the isocyanate **3** (1.0 mmol) in EtOAc (60 mL) was added to the reaction mixture and stirred for 2 h at room temperature. The reaction mixture was

acidified with diluted HCl to pH 3 and twice extracted with EtOAc (60 mL). The combined organic layer was washed twice with water (2 × 30 mL), dried over anhydrous Na_2SO_4, filtered and concentrated under the reduced pressure. The residue **4** was added methanol (30 mL) and NaOH (20 mmol), and the reaction mixture was stirred at room temperature for 12 h. Water (50 mL) was added and the pH was adjusted to 3 using diluted HCl. The reaction mixture was twice extracted with EtOAc (2 × 60 mL). The combined organic phase was washed twice with water (2 × 30 mL), dried over anhydrous Na_2SO_4, filtered and concentrated under the reduced pressure. The residue was purified by flash chromatography (SiO_2, MeOH-CH_2Cl_2, gradient elution) to give the urea product **5**.

*4.3.1. 1-((3β,20β)-3-acetoxyl-11-oxo-olean-12-en-20-yl)-3-(acetic acid-2-yl)urea (**4a**)*

Method B; white powder, 72%; m.p. 213–215 °C; ^{1}H NMR (400 MHz, DMSO-d_6) δ 5.90 (t, J = 5.7 Hz, 1H, CH_2*NH*), 5.85 (s, 1H, NH), 5.50 (s, 1H, 12-H), 4.42 (dd, J = 11.8, 4.5 Hz, 1H, 3-H), 3.71 (dd, J = 18.0, 4.9 Hz, 1H, NCH_2-Ha), 3.63 (dd, J = 18.0, 4.5 Hz, 1H, NCH_2-Hb), 2.63 (m, 1H, 9-H), 2.38 (s, 1H, 18-H), 2.20–2.08 (m, 2H), 2.00 (s, 3H, CH_3CO), 1.88–1.35 (m, 12H), 1.34 (s, 3H, 29-H), 1.20 (s, 3H, 27-H), 1.13 (m, 3H), 1.06, 1.04 (2 × s, 2 × 3H, 23-H, 24-H), 0.90 (m, 2H), 0.82 (s, 6H, 25-H, 28-H), 0.79 (s, 3H, 26-H); ^{13}C NMR (100 MHz, DMSO-d_6) δ 199.1 (C-11), 172.7 (COOH), 170.3 (C-13), 170.2 (CH_3*CO*), 157.2 (C-30), 127.1 (C-12), 79.7 (C-3), 60.8 (C-9), 53.7 (C-20), 51.4 (C-5), 45.9 (C-18), 44.9 (C-19), 43.0 (NCH_2), 42.1 (C-14), 41.4 (C-8), 37.9 (C-4), 37.6 (C-1), 36.5 (C-10), 35.3 (C-16), 31.9 (C-17), 31.5 (C-7), 31.3 (C-22), 28.4 (C-29), 28.3 (C-23), 27.7 (C-28), 26.1 (C-21), 25.8 (C-2), 23.2 (C-15), 23.0 (C-27), 21.0 (*CH*$_3$CO), 18.4 (C-25), 17.0 (C-6), 16.6 (C-24), 16.2 (C-26). TOF-HRMS: m/z $[M + H]^+$ calcd for $C_{34}H_{53}N_2O_6$: 585.4341; found: 585.4340.

*4.3.2. 1-((3β,20β)-3-hydroxyl-11-oxo-olean-12-en-20-yl)-3-(acetic acid-2-yl)urea (**5a**)*

Method B; white powder, 65%; m.p. 221–223 °C; ^{1}H NMR (400 MHz, DMSO-d_6) δ 5.91 (t, J = 5.6 Hz, 1H, *NH*CH_2), 5.85 (s, 1H, NH), 5.49 (s, 1H, 12-H), 4.33 (brs, 1H, OH), 3.70 (dd, J = 17.9, 4.8 Hz, 1H, NCH_2-Ha), 3.62 (dd, J = 18.0, 4.5 Hz, 1H, NCH_2-Hb), 3.01 (dd, J = 17.2, 4.4 Hz, 1H, 3-H), 2.57 (m, 1H, 9-H), 2.30 (s, 1H, 18-H), 2.19–1.33 (m, 14H), 1.32 (s, 3H, 29-H), 1.20 (s, 3H, 27-H), 1.14 (m, 2H), 1.03, 1.02 (2 × s, 2 × 3H, 23-H, 24-H), 0.93 (m, 2H), 0.90 (s, 3H, 25-H), 0.79 (s, 3H, 28-H), 0.69 (, 1H), 0.68 (s, 3H, 26-H); ^{13}C NMR (100 MHz, DMSO-d_6) δ 199.2 (C-11), 172.7 (COOH), 170.1 (C-13), 157.2 (C-30), 127.2 (C-12), 77.6 (C-3), 61.2 (C-9), 54.1 (C-20), 51.4 (C-5), 45.9 (C-18), 44.9 (C-19), 43.0 (NCH_2), 42.1 (C-14), 41.4 (C-8), 38.8 (C-4), 38.6 (C-1), 36.7 (C-10), 35.4 (C-16), 32.1 (C-17), 31.5 (C-7), 31.3 (C-22), 28.4 (C-29), 28.3 (C-23), 28.2 (C-28), 27.0 (C-21), 26.1 (C-15), 25.6 (C-2), 23.0 (C-27), 18.4 (C-25), 17.2 (C-6), 16.2 (C-26), 16.0 (C-24). TOF-HRMS: m/z $[M + H]^+$ calcd for $C_{32}H_{51}N_2O_5$: 543.4228; found: 543.4230.

*4.3.3. 1-((3β,20β)-3-hydroxyl-11-oxo-olean-12-en-20-yl)-3-(methyl acetate-2-yl)urea (**5b**)*

Method B; white powder, 51%; m.p. 226–228 °C; ^{1}H NMR (400 MHz, DMSO-d_6) δ 6.00 (t, J = 6.1 Hz, 1H, CH_2*NH*), 5.87 (s, 1H, NH), 5.49 (s, 1H, 12-H), 4.32 (d, J = 5.2 Hz, 1H, OH), 3.78 (dd, J = 17.8, 6.2 Hz, 1H, NCH_2-Ha), 3.71 (dd, J = 17.8, 5.9 Hz, 1H, NCH_2-Hb), 3.62 (s, 3H, OCH_3), 3.01 (m, 2H, 3-H), 2.58 (m, 1H, 9-H), 2.30 (s, 1H, 18-H), 2.13 (m, 2H), 1.84–1.34 (m, 12H), 1.32 (s, 3H, 29-H), 1.19 (s, 3H, 27-H), 1.14 (m, 2H), 1.04, 1.02 (2 × s, 2 × 3H, 23-H, 24-H), 0.95 (m, 2H), 0.90 (s, 3H, 25-H), 0.79 (s, 3H, 28-H), 0.68 (s, 3H, 26-H), 0.68 (m, 1H); ^{13}C NMR (100 MHz, DMSO-d_6) δ 199.2 (C-11), 171.9 (COO), 170.1 (C-13), 157.2 (C-30), 127.2 (C-12), 76.6 (C-3), 61.1 (C-9), 54.1 (C-20), 51.5 (C-5), 51.4 (OCH_3), 45.9 (C-18), 44.9 (C-19), 42.9 (NCH_2), 41.8 (C-14), 41.2 (C-8), 38.8 (C-4), 38.5 (C-1), 36.7 (C-10), 35.3 (C-16), 32.1 (C-17), 31.5 (C-7), 31.4 (C-22), 28.4 (C-29), 28.3 (C-23), 28.2 (C-28), 27.0 (C-21), 26.1 (C-15), 25.8 (C-2), 23.0 (C-27), 18.4 (C-25), 17.2 (C-6), 16.2 (C-26), 16.0 (C-24). TOF-HRMS: m/z $[M + H]^+$ calcd for for $C_{33}H_{53}N_2O_5$: 557.4400; found: 557.4404.

*4.3.4. 1-((3β,20β)-3-hydroxyl-11-oxo-olean-12-en-20-yl)urea (**5c**)*

Mehtod A; white powder, 80%; m.p. 228–230 °C; ^{1}H NMR (500 MHz, DMSO-d_6) δ 5.60 (s, 1H, CO*NH*), 5.46 (s, 1H, 12-H), 5.21 (s, 2H, NH_2), 4.30 (d, J = 5.2 Hz, 1H, OH), 3.01 (m, 1H, 3-H), 2.58 (m, 1H, 9-H), 2.30 (s, 1H, 18-H), 2.10 (m, 2H), 1.87–1.36 (m, 14H), 1.32 (s, 3H, 29-H), 1.19 (s, 3H, 27-H), 1.14 (m, 2H), 1.04, 1.02 (2 × s, 2 × 3H, 23-H, 24-H), 0.94 (m, 2H), 0.90 (s, 3H, 25-H), 0.80 (s, 3H, 28-H), 0.69 (s, 1H), 0.68 (s, 3H, 26-H); ^{13}C NMR (126 MHz, DMSO-d_6) δ 199.0 (C-11), 170.0 (C-13), 158.1 (C-30), 127.1 (C-12), 76.5 (C-3), 61.1 (C-9), 54.1 (C-20), 51.1 (C-5), 46.0 (C-18), 44.8 (C-19), 42.9 (C-14), 41.9 (C-8), 38.8 (C-4), 38.5 (C-1), 36.6 (C-10), 35.4 (C-16), 32.1 (C-17), 31.5 (C-7), 31.4 (C-22), 28.3 (C-29), 28.3 (C-23), 28.1 (C-28), 26.9 (C-21), 25.8 (C-15), 22.9 (C-2), 18.4 (C-27), 17.1 (C-25), 17.0 (C-6), 16.2 (C-26), 16.0 (C-24). TOF-HRMS: m/z $[M + H]^+$ calcd for $C_{30}H_{49}N_2O_3$: 485.4148; found: 485.4149.

*4.3.5. 1-((3β,20β)-3-acetoxyl-11-oxo-olean-12-en-20-yl)-3-hydroxylurea (**4d**)*

Method B; white powder, 67%; m.p. 231–233 °C; ^{1}H NMR (400 MHz, DMSO-d_6) δ 8.63 (s, 1H, NHO*H*), 8.17 (s, 1H, *NH*OH), 5.82 (s, 1H, CO*NH*), 5.47 (s, 1H, 12-H), 4.30 (dd, J = 11.8, 4.5 Hz, 1H, 3-H), 2.63 (m, 1H, 9-H), 2.39 (s, 1H, 18-H), 2.05 (m, 3H), 2.00 (s, 3H, $COCH_3$), 1.92–1.14 (m, 10*H*), 1.35 (s, 3H, 29-H), 1.23 (m, 5H, overlap 27-H), 1.14 (m, 2H), 1.06, 1.04 (2 × s, 2 × 3H, 23-H, 24-H), 0.92 (m, 2H), 0.82 (s, 6H, 25-H, 28-H), 0.80 (s, 3H, 26-H). TOF-HRMS: m/z $[M + H]^+$ calcd for $C_{32}H_{51}N_2O_5$: 543.4326; found: 543.4324.

*4.3.6. 1-((3β,20β)-3-acetoxyl-11-oxo-olean-12-en-20-yl)-3-(2-hydroxyethyl)urea (**4e**)*

Method A; white powder, 77%; m.p. 224–227 °C; ^{1}H NMR (400 MHz, DMSO-d_6) δ 5.76 (t, J = 5.6 Hz, 1H, *NH*CH_2), 5.65 (s, 1H, 12-H), 5.48 (s, 1H, CONH), 4.70 (t, J = 5.0 Hz, 1H, 3-H), 4.42 (dd, J = 11.8, 4.5 Hz, 1H, OH), 3.37 (m, 2H, *CH*$_2$OH), 3.02 (m, 2H, NH*CH*$_2$), 2.63 (m, 1H, 9-H), 2.39 (s, 1H, 18-H), 2.10 (m, 1H), 2.00 (s, 3H, OCH_3), 1.90 (d, J = 13.2 Hz, 1H), 1.76–1.36 (m, 10*H*), 1.34 (s, 3H, 29-H), 1.20 (s, 3H, 27-H), 1.06, 1.04 (2 × s, 2 × 3H, 23-H, 24-H), 0.90 (m, 2H), 0.82 (s, 6H, 25-H, 28-H), 0.79 (s, 3H, 26-H). TOF-HRMS: m/z $[M + H]^+$ calcd for $C_{34}H_{55}N_2O_5$: 571.4322; found: 571.4318.

*4.3.7. 1-((3β,20β)-3-hydroxyl-11-oxo-olean-12-en-20-yl)-3-(2-hydroxyethyl)urea (**5e**)*

Method **A**; white powder, 66%; m.p. 229–230 °C; ^{1}H NMR (400 MHz, DMSO-d_6) δ 5.76 (t, J = 5.5 Hz, 1H, CH_2*NH*), 5.65 (s, 1H, 12-H), 5.47 (s, 1H, NH), 4.70 (t, J = 5.0 Hz, 1H,CH_2*OH*), 4.32 (d, J = 5.1 Hz, 1H, OH), 3.37 (m, 2H, *CH*$_2$OH), 3.01 (m, 3H, 3-H), 2.57 (d, J = 13.3 Hz, 1H, 9-H), 2.30 (s, 1H, 18-H), 2.15 (m, 2H, NH*CH*$_2$), 1.89 (d, J = 12.7 Hz, 3H), 1.79–1.35 (m, 11*H*), 1.31 (d, J = 13.8 Hz, 3H, 29-H), 1.20 (s, 3H), 1.15 (m, 2H), 1.03, 1.02 (2 × s, 2 × 3H, 23-H, 24-H), 0.94 (s, 2H), 0.90 (s, 3H, 25-H), 0.78 (s, 3H, 28-H), 0.70 (s, 1H), 0.68 (s, 3H, 26-H); ^{13}C NMR (101 MHz, DMSO) δ 199.1 (C-11), 170.1 (C-13), 157.5 (C-30), 127.1 (C-12), 76.6 (C-3), 61.1 (C-9), 60.9 (CH_2OH), 54.1 (C-20), 51.2 (C-5), 45.9 (C-18), 44.9 (C-19), 42.9 (C-14), 42.4 (C-8), 41.7 (C-4), 38.8 (C-1), 38.5 (C-10), 36.7 (C-16), 35.4 (C-17), 32.1 (NCH_2), 31.5 (C-7), 31.2 (C-22), 28.4 (C-29), 28.3 (C-23), 28.1 (C-28), 27.0 (C-21), 26.0 (C-15), 25.8 (C-2), 23.0 (C-27), 18.36 (C-25), 17.2 (C-6), 16.2 (C-26), 16.0 (C-24). TOF-HRMS: m/z $[M + H]^+$ calcd for $C_{32}H_{53}N_2O_4$: 529.4312; found: 529.4315.

*4.3.8. N-((3β,20β)-3-hydroxyl-11-oxo-olean-12-en-20-yl)piperazidine-1-carboxamide (**5f**)*

Mehtod A; white powder, 72%; m.p. 169–171 °C; ^{1}H NMR (400 MHz, DMSO-d_6) δ 5.64 (s, 1H, CO*NH*), 5.60 (s, 1H, 12-H), 4.32 (d, J = 5.1 Hz, 1H, OH), 3.27 (t, J = 5.0 Hz, 4H, piperazine), 3.01 (m, 2H, 3-H), 2.58 (m, 1H, 9-H), 2.30 (s, 1H, 18-H), 2.23 (t, J = 5.0 Hz, 4H, piperazine),

2.15 (s, 3H, NCH_3), 2.12–1.90 (m, 15H), 1.87–1.22 (m, 12H, overlap 1.31, s, 3H, 29-H), 1.20 (s, 3H, 27-H), 1.17–1.06 (m, 3H), 1.03, 1.02 (2 × s, 2 × 3H, 23-H, 24-H), 0.95 (m, 2H), 0.90 (s, 3H, 25-H), 0.78 (s, 3H, 28-H), 0.70 (s, 1H), 0.68 (s, 3H, 26-H); ^{13}C NMR (101 MHz, DMSO-d_6) δ 199.2 (C-11), 169.9 (C-13), 157.0 (C-30), 127.4 (C-12), 76.6 (C-3), 61.1 (C-9), 54.7 (2C, piperazine), 54.1 (C-20), 52.1 (C-5), 46.0 (C-18), 45.9 (2C, piperazine), 44.8 (C-19), 44.1 (NCH_3), 43.0 (C-14), 41.7 (C-8), 38.8 (C-4), 38.6 (C-1), 36.7 (C-10), 35.7 (C-16), 32.1 (C-17), 31.4 (C-7), 30.8 (C-22), 28.6 (C-29), 28.3 (C-23), 28.1 (C-28), 26.9 (C-21), 26.1 (C-15), 26.0 (C-2), 22.9 (C-27), 18.3 (C-25), 17.2 (C-6), 16.2 (C-26), 16.0 (C-24). TOF-HRMS: *m/z* $[M + H]^+$ calcd for $C_{35}H_{58}N_3O_3$: 568.4432; found: 568.4428.

4.3.9. N-((3β,20β)-3-hydroxyl-11-oxo-olean-12-en-20-yl)piperidine-1-carboxamide (5 g)

Method A; white powder, 78%; m.p. 157–159 °C; ^{1}H NMR (400 MHz, DMSO-d_6) δ 5.57 (s, 1H, CONH), 5.56 (s, 1H, 12-H), 4.37 (brs, 1H, OH), 3.24 (m, 4H, piperidine), 3.01 (m, 1H, 3-H), 2.58 (m, 1H, 9-H), 2.31 (s, 1H, 18-H), 2.10 (m, 4H), 1.76–1.34 (m, 16H), 1.32 (s, 3H, 29-H), 1.19 (s, 3H, 27-H), 1.15 (m, 2H), 1.03, 1.02 (2 × s, 2 × 3H, 23-H, 24-H), 0.94 (s, 2H), 0.90 (s, 3H, 25-H), 0.78 (s, 3H, 28-H), 0.70 (m, 1H), 0.68 (s, 3H, 26-H); ^{13}C NMR (101 MHz, DMSO-d_6) δ 199.4 (C-11), 170.2 (C-13), 157.1 (C-30), 127.4 (C-12), 76.7 (C-3), 61.2 (C-9), 54.2 (C-20), 52.1 (C-5), 46.3 (2C, piperidine), 45.3 (C-18), 44.9 (C-19), 43.1 (C-14), 41.6 (C-8), 38.9 (C-4), 38.7 (C-1), 36.8 (C-10), 35.9 (C-16), 32.3 (C-17), 31.5 (C-7), 31.2 (C-22), 28.7 (C-29), 28.5 (C-23), 28.2 (C-28), 27.0 (C-21), 26.2 (C-15), 26.1 (C-2), 25.6 (2C, piperidine), 24.4 (piperidine), 23.0 (C-27), 18.4 (C-25), 17.3 (C-6), 16.3 (C-26), 16.1 (C-24). TOF-HRMS: *m/z* $[M + H]^+$ calcd for $C_{35}H_{57}N_2O_3$: 553.4849; found: 553.4848.

4.3.10. N-((3β,20β)-3-hydroxyl-11-oxo-olean-12-en-20-yl)morpholine-4-carboxamide (5 h)

Method A; white powder, 80%; m.p. 226–228 °C; ^{1}HNMR (400 MHz, DMSO-d_6) δ 5.69 (s, 1H, CONH), 5.59 (s, 1H,12-H), 4.36 (brs ,1H, OH), 3.55–3.52 (m, 4H, morpholine), 3.22 (dd, J = 5.8, 3.9 Hz, 4H, morpholine), 3.01 (m, 1H, 3-H), 2.58 (m, 1H, 9-H), 2.30 (s, 1H,18-H), 2.07 (m, 2H), 1.81–1.34 (m, 12H), 1.31 (s, 3H, 29-H), 1.20 (s, 3H, 29-H), 1.14 (m, 2H), 1.02, 1.01 (2 × s, 2 × 3H, 23-H, 24-H), 0.93 (m, 2H), 0.89 (s, 3H, 25-H), 0.77 (s, 3H, 28-H), 0.70 (s, 1H), 0.68 (s, 3H, 26-H); ^{13}C NMR (101 MHz, DMSO-d_6) δ 199.4 (C-11), 170.1 (C-13), 157.4 (C-30), 127.5 (C-12), 76.7 (C-3), 66.2 (2C, morpholine), 61.2 (C-9), 54.2 (C-20), 52.2 (C-5), 46.1 (C-18), 44.9 (C-19), 44.8 (2C, morpholine), 43.1 (C-14), 41.8 (C-8), 38.9 (C-4), 38.7 (C-1), 36.8 (C-10), 35.8 (C-16), 32.2 (C-17), 31.5 (C-7), 30.8 (C-22), 28.7 (C-29), 28.3 (C-23), 28.2 (C-28), 27.0 (C-21), 26.1 (C-15), 26.1 (C-2), 23.0 (C-27), 18.4 (C-25), 17.3 (C-6), 16.3 (C-26), 16.1 (C-24). TOF-HRMS: *m/z* $[M + H]^+$ calcd for $C_{34}H_{55}N_2O_4$: 555.4156; found: 555.4154.

4.3.11. N-((3β,20β)-3-hydroxyl-11-oxo-olean-12-en-20-yl)pyrrolidine-1-carboxamide (5i)

Method A; white powder, 77%; m.p. 220–222 °C; ^{1}HNMR (400 MHz, DMSO-d_6) δ 5.57 (s, 1H, CONH), 4.95 (s, 1H, 12-H), 4.36 (d, J = 5.2 Hz, 1H, OH), 3.20 (m, 4H, pyrrolidine), 3.01 (m, 1H, 3-H), 2.58 (m, 1H, 9-H), 2.30 (s, 1H, 18-H), 2.07 (m, 4H, pyrrolidine), 1.76 (m, 5H), 1.63–1.35 (m, 12H), 1.31 (s, 3H, 29-H) 1.20 (s, 3H, 27-H), 1.15 (m, 2H), 1.02,1.01 (2 × s, 2 × 3H, 23-H, 24-H), 0.93 (m, 2H), 0.89 (s, 3H, 25-H), 0.78 (s, 3H, 28-H), 0.70 (s, 1H), 0.68 (s, 3H, 26-H); ^{13}C NMR (101 MHz, DMSO-d_6) δ 199.4 (C-11), 170.1 (C-13), 157.4 (C-30), 127.5 (C-12), 76.7 (C-3), 61.2 (C-9), 54.2 (C-20), 52.2 (C-5) 46.1 (C-18), 44.9 (C-19), 44.8 (2C, pyrrolidine), 43.1 (C-14), 41.8 (C-8), 38.9 (C-4), 38.7 (C-1), 36.8 (C-10), 35.8 (C-16), 32.2 (C-17), 31.5 (C-7, C-22), 30.8 (C-29), 28.7 (C-23), 28.3 (C-28), 28.2 (C-21), 27.0 (C-15), 26.1 (C-2), 26.0 (2C, pyrrolidine), 23.0 (C-27), 18.4 (C-25), 17.3 (C-6), 16.3 (C-26), 16.1 (C-24). TOF-HRMS: *m/z* $[M + H]^+$ calcd for $C_{34}H_{55}N_2O_3$: 539.4415; found:539.4413.

4.3.12. 1-((3β,20β)-3-hydroxyl-11-oxo-olean-12-en-20-yl)-3-(3-pyridylmethyl)urea (5j)

Method A; white powder, 70%; m.p. 227–229 °C; ^{1}HNMR (400 MHz, DMSO-d_6) δ 8.45 (dd, J = 2.3, 0.9 Hz, 1H), 8.43 (dd, J = 4.8, 1.7 Hz, 1H), 7.64 (m, 1H), 7.34 (m, 1H), 6.23 (t, J = 6.1 Hz, 1H, *NH*CH_2), 5.69 (s, 1H, NH), 5.42 (s, 1H, 12-H), 4.36 (d, J = 5.1 Hz, 1H, OH), 4.20 (m, 2H, *CH*$_2$NH), 3.00 (m, 2H, 3-H), 2.56 (m, 1H, 9-H), 2.30 (s, 1H, 18-H), 2.08 (m, 2H), 1.86–1.35 (m, 12H), 1.31 (s, 3H, 29-H), 1.22 (s, 3H, 27-H), 1.14 (m, 2H), 1.03, 1.02 (2 × s, 2 × 3H, 23-H, 24-H), 0.93 (s, 2H), 0.89 (s, 3H, 25-H), 0.78 (s, 3H, 28-H), 0.69 (s, 1H), 0.68 (s, 3H, 26-H); ^{13}C NMR (101 MHz, DMSO-d_6) δ 199.3 (C-11), 170.1 (C-13), 157.4 (C-30), 148.5 (pyridine), 147.9 (pyridine), 136.7 (pyridine), 134.8 (pyridine), 127.2 (C-12), 123.5 (pyridine), 76.7 (C-3), 61.2 (C-9), 54.2 (C-20), 51.6 (C-5), 46.2 (C-18), 45.0 (C-19), 43.1 (NCH_2), 41.9 (C-14), 40.4 (C-8), 40.1 (C-4), 38.9 (C-1), 38.6 (C-10), 36.7 (C-16), 35.5 (C-17), 32.2 (C-7), 31.6 (C-22), 28.5 (C-29), 28.4 (C-23), 28.2 (C-28), 27.0 (C-21), 26.1 (C-15), 25.9 (C-2), 23.0 (C-27), 18.5 (C-25), 17.3 (C-6), 16.3 (C-26), 16.1 (C-24). TOF-HRMS: *m/z* $[M + H]^+$ calcd for $C_{36}H_{54}N_3O_3$: 576.4540; found: 576.4538.

4.3.13. 1-((3β,20β)-3-hydroxyl-11-oxo-olean-12-en-20-yl)-3-(4-pyridylmethyl)urea (5 k)

Method A; white powder, 71%; m.p. 228–230 °C; ^{1}H NMR (400 MHz, DMSO-d_6) δ 8.48 (m, 1H), 7.23 (d, J = 5.8 Hz, 2H), 6.28 (t, J = 6.1 Hz, 1H, *NH*CH_2), 5.76 (s, 1H, 12-H), 5.45 (s, 1H, CO*NH*), 4.32 (d, J = 5.1 Hz, 1H, OH), 4.20 (m, 1H), 3.00 (m, 1H, 3-H), 2.58 (m, 1H, 9-H), 2.31 (s, 1H, 18-H), 2.11 (m, 2H), 1.88–1.35 (m, 18H), 1.32 (s, 3H, 27-H), 1.23 (s, 3H), 1.15 (m, 3H), 1.04, 1.03 (2 × s, 2 × 3H, 23-H, 24-H), 0.92 (m, 2H), 0.90 (s, 3H, 25-H), 0.80 (s, 3H, 28-H), 0.70 (m, 1H), 0.68 (s, 3H, 26-H); ^{13}C NMR (101 MHz, DMSO) δ 199.1 (C-11), 170.0 (C-13), 157.3 (C-30), 150.5 (pyridine), 149.4 (2C, pyridine), 127.1 (C-12), 121.8 (2C, pyridine), 76.6 (C-3), 61.1 (C-9), 54.1 (C-20), 51.5 (C-5), 46.2 (C-18), 44.9 (C-19), 43.0 (NCH_2), 41.7 (C-14), 41.6 (C-8), 38.8 (C-4), 38.5 (C-1), 36.6 (C-10), 35.4 (C-16), 32.1 (C-17), 31.6 (C-27), 31.5 (C-22), 28.4 (C-29), 28.3 (C-23), 28.2 (C-28), 27.0 (C-21), 26.1 (C-15), 25.8 (C-2), 22.9 (C-27), 18.4 (C-25), 17.2 (C-6), 16.2 (C-26), 16.0 (C-24). TOF-HRMS: *m/z* $[M + H]^+$ calcd for $C_{36}H_{54}N_3O_3$: 576.4606; found: 576.4608.

4.3.14. 1-((3β,20β)-3-hydroxyl-11-oxo-olean-12-en-20-yl)-3-methylurea (5 l)

Method B; white powder, 75%; m.p. 187–189 °C; ^{1}H NMR (400 MHz, DMSO-d_6) δ 6.25 (t, J = 4.0 Hz, 1H, CH_3*NH*), 5.94 (s, 1H, NH), 5.59 (s, 1H, 12-H), 5.82 (brs, 1H, OH), 3.50 (dd, J = 11.3, 4.0 Hz, 1H, 3-H), 3.18 (m, 1H, 9-H), 2.88 (d, J = 4.6 Hz, 3H, NCH_3), 2.47 (s, 1H, 18-H), 2.35 (m, 2H), 2.12–1.62 (m, 8H), 1.60 (s, 3H, 29-H), 1.47 (m, 2H), 1.33 (s, 3H, 27-H), 1.23 (m, 3H), 1.03, 1.02 (2 × s, 2 × 3H, 23-H, 24-H), 1.06 (m, 2H), 1.11 (s, 3H, 25-H), 1.09 (s, 3H, 28-H), 0.88 (m, 2H), 0.83 (s, 3H, 26-H); ^{13}C NMR (100 MHz, DMSO-d_6) δ 200.0 (C-11), 170.0 (C-13), 159.8 (C-30), 128.8 (C-12), 78.3 (C-3), 62.6 (C-9), 55.7 (C-20), 52.9 (C-5), 47.5 (C-18), 46.0 (C-19), 44.0 (C-14), 43.6 (C-10), 40.2 (C-8, C-4), 38.1 (C-1), 36.7 (C-16), 33.4 (C-17), 32.7 (C-7), 32.5 (NCH_3), 28.6 (C-22), 29.6 (C-29), 29.2 (C-23), 29.1 (C-28), 27.3 (C-21), 27.1 (C-15), 27.0 (C-2), 23.8 (C-27), 19.3 (C-25), 18.4 (C-6), 17.3 (C-26), 17.1 (C-24). TOF-HRMS: *m/z* $[M + H]^+$ calcd for $C_{31}H_{51}N_2O_3$: 449.3894; found: 449.3899.

4.3.15. 1-((3β,20β)-3-hydroxyl-11-oxo-olean-12-en-20-yl)-3-ethylurea (5 m)

Mehtod B; white powder, 81%; m.p. 220–223 °C; ^{1}H NMR (400 MHz, DMSO-d_6) δ 5.60 (t, J = 5.5 Hz, 1H, *NH*CH_2), 5.45 (s, 2H, CONH, 12-H), 4.37 (d, J = 5.2 Hz, 1H, OH), 2.98 (m, 4H, 3-H), 2.56 (m, 1H, 9-H), 2.30 (s, 1H, 18-H), 2.08 (m, 2H), 1.92–1.33 (m, 11*H*), 1.31 (s, 3H, 29-H) 1.19 (s, 5H), 1.03, 1.01 (2 × s, 2 × 3H, 23-H, 24-H), 0.97 (t, J = 7.2 Hz, 3H), 0.93 (s, 1H), 0.89 (s, 3H, 25-H), 0.78 (s, 3H, 28-H), 0.69 (s, 1H), 0.68 (s, 3H, 26-H); ^{13}C NMR (101 MHz, DMSO-d_6) δ 199.3 (C-11), 170.3 (C-13), 157.5 (C-30), 127.2 (C-12), 76.7 (C-3), 61.2 (C-9), 54.2 (C-20), 51.4 (C-

5), 46.1 (C-18), 45.0 (C-19), 43.1 (C-14), 42.3 (C-8), 38.9 (C-4), 38.6 (C-1), 36.7 (C-10), 35.5 (C-16), 33.9 (C-17), 32.2 (C-7), 31.6 (C-22), 31.5 (NCH_2), 28.6 (C-29), 28.4 (C-23), 28.2 (C-28), 27.0 (C-21), 26.1 (C-15), 25.9 (C-2), 23.1 (C-27), 18.5 (C-25), 17.3 (C-6), 16.3 (C-26), 16.1 (C-24), 15.8 (CH_2CH_3). TOF-HRMS: *m/z* $[M + H]^+$ calcd for $C_{32}H_{53}N_2O_3$: 513.4051; found: 513.4048.

4.3.16. 1-((3β,20β)-3-hydroxyl-11-oxo-olean-12-en-20-yl)-3-isopropylurea (5n)

Mehtod B; white powder, 80%; m.p. 224–226 °C; ^{1}H NMR (400 MHz, DMSO-d_6) δ 5.50 (d, $J = 7.8$ Hz, 1H, CH*NH*), 5.44 (s, 1H, 12-H), 5.38 (s, 1H, NH), 4.32 (d, $J = 5.2$ Hz, 1H, OH), 3.60 (m, 1H), 3.0(m, 1H, 3-H) 2.57 (m, 1H, 9-H), 2.30 (s, 1H, 18-H), 2.08 (m, 2H), 1.84–1.34 (m, 12H), 1.31 (s, 3H, 29-H), 1.20 (s, 3H), 1.15 (m, 3H), 1.07–1.00 (m, 12H, 23-H, 24-H, NH*(CH$_2$)$_3$*), 0.93 (m, 2H), 0.90 (s, 3H, 25-H), 0.79 (s, 3H, 28-H), 0.70 (s, 1H), 0.68 (s, 3H, 26-H); ^{13}C NMR (101 MHz, DMSO) δ 199.1 (C-11), 170.1 (C-13), 156.8 (C-30), 127.1 (C-12), 76.6 (C-3), 61.1 (C-9), 54.1 (C-20), 51.2 (C-5), 46.1 (C-18), 44.9 (C-19), 43.0 (C-14), 42.1 (C-8), 40.6 (NH*CH)*, 38.8 (C-4), 38.5 (C-1), 36.7 (C-10), 35.4 (C-16), 32.1 (C-17), 31.5 (C-7, C-22), 28.5 (C-29), 28.3 (C-23), 28.1 (C-28), 27.0 (C-21), 26.0 (C-15), 25.8 (C-2), 23.3 (CH*CH$_3$*), 23.2 (CH*CH$_3$*), 23.0 (C-27), 18.4 (C-25), 17.2 (C-6), 16.2 (C-26), 16.0 (C-24). TOF-HRMS: *m/z* $[M + H]^+$ calcd for $C_{33}H_{55}N_2O_3$: 527.4640; found: 527.4639.

4.3.17. 1-((3β,20β)-3-hydroxyl-11-oxo-olean-12-en-20-yl)-3-n-butylurea (5o)

Mehtod A; white powder, 76%; m.p. 227–230 °C; ^{1}H NMR (400 MHz, DMSO-d_6) δ 5.63 (t, $J = 5.5$ Hz, 1H, *NH*CH_2), 5.44 (s, 2H, CONH, 12-H), 4.37 (d, $J = 5.2$ Hz, 1H, OH), 3.00 (m, 3H, 3-H), 2.56 (m, 1H, 9-H), 2.30 (s, 1H, 18-H), 2.08 (m, 6.5 Hz, 2H), 1.92–1.34 (m, 11*H*), 1.31 (s, 3H, 27-H) 1.19 (s, 5H), 1.02, 1.01 (2 × s, 2 × 3H, 23-H, 24-H), 0.93 (m, 2H), 0.89 (s, 3H, 25-H), 0.86 (t, $J = 7.2$ Hz, 3H, CH_2CH_3), 0.78 (s, 3H, 28-H), 0.69 (s, 1H), 0.68 (s, 3H, 26-H); ^{13}C NMR (101 MHz, DMSO-d_6) δ 199.3 (C-11), 170.3 (C-13), 157.6 (C-30), 127.2 (C-12), 76.7 (C-3), 61.2 (C-9), 54.2 (C-20), 51.3 (C-5), 46.2 (C-18), 45.0 (C-19), 43.1 (C-14), 42.1 (C-8), 38.9 (C-4), 38.6 (C-1), 38.6 (NCH_2), 36.7 (C-10), 35.5 (C-16), 32.3 (C-17), 32.2 (C-7), 31.6 (C-22), 31.6 (NCH_2CH_2), 28.6 (C-29), 28.4 (C-23), 28.2 (C-28), 27.0 (C-21), 26.1 (C-15), 25.9 (C-2), 23.0 (C-27), 19.6 (CH_2CH_3), 18.5 (C-25), 17.3 (C-6), 16.3 (C-26), 16.1 (C-24), 13.8 (CH_2CH_3). TOF-HRMS: *m/z* $[M + H]^+$ calcd for $C_{34}H_{57}N_2O_3$: 541.4364; found: 541.4359.

4.3.18. 1-((3β,20β)-3-hydroxyl-11-oxo-olean-12-en-20-yl)-3-dimethylurea (5p)

Mehtod B; white powder, 65%; m.p. 151–153 °C; ^{1}H NMR (400 MHz, $CDCl_3$) δ 5.56 (s, 1H, CO*NH*), 4.03 (s, 1H,12-H), 3.18 (m, 1H, 3-H), 2.86 (s, 6H, NH*(CH$_3$)$_2$*), 2.72 (m, 1H, 9-H), 2.30 (m, 1H, 18-H), 2.04 (m, 3H), 1.84–1.54 (m, 10*H*), 1.42–1.27 (m, 12H) 1.16 (m, 1H), 1.10, 1.09 (2 × s, 2 × 3H, 23-H, 24-H), 1.00 (m, 2H), 0.97 (s, 3H, 25-H), 0.83 (s, 3H, 28-H), 0.77 (s, 3H, 26-H), 0.66 (m, 1H); ^{13}C NMR (101 MHz, $CDCl_3$) δ 200.3 (C-11), 169.1 (C-13), 157.5 (C-30), 128.6 (C-12), 78.9 (C-3), 62.0 (C-9), 55.1 (C-20), 52.9 (C-5), 47.4 (C-18), 45.6 (C-19), 43.5 (C-14), 43.0 (C-8), 39.3 (C-4), 39.3 (C-1), 37.2 (C-10), 36.6 (C-16), 36.1 ($N(CH_3)_2$), 33.0 (C-17), 32.2 (C-7), 32.0 (C-22), 28.9 (C-29), 28.8 (C-23), 28.3 (C-28), 27.4 (C-21), 26.6 (C-15), 26.5 (C-2), 23.5 (C-27), 18.8 (C-25), 17.7 (C-6), 16.6 (C-26), 15.8 (C-24). $C_{32}H_{53}N_2O_3$: 513.4240; found: 513.4235.

4.3.19. 1-((3β,20β)-3-hydroxyl-11-oxo-olean-12-en-20-yl)-3-(2-dimethylaminoethyl-1-yl)urea (5q)

Mehtod A; white powder, 60%; m.p. 228–230 °C; ^{1}H NMR (400 MHz, DMSO-d_6) δ 5.70 (s, 1H, CO*NH*), 5.65 (t, $J = 5.4$ Hz, 1H, *NH*CH_2), 5.48 (s, 1H, 12-H), 4.37 (d, $J = 5.2$ Hz, 1H, OH), 3.02 (m, 1H ,3-H), 2.56 (m, 1H, 9-H), 2.30 (s, 1H, 18-H), 2.23 (t, $J = 6.2$ Hz, 2H, $NHCH_2CH_2$), 2.13 (s, 8H), 2.07–1.33 (m, 13H), 1.31 (s, 3H, 29-H), 1.18 (s, 3H, 28-H), 1.15 (m, 2H), 1.03, 1.02 (2 × s, 2 × 3H, 23-H, 24-H), 0.93 (s, 2H), 0.89 (s, 3H, 25-H), 0.78 (s, 3H, 28-H), 0.69 (s, 1H), 0.68 (s, 3H, 26-H); ^{13}C NMR (101 MHz, DMSO-d_6) δ 199.3 (C-11), 170.3 (C-13), 157.5 (C-30), 127.2 (C-12), 76.7 (C-3), 61.2 (C-9), 59.1 (NCH_2), 54.2 (C-20), 51.4 (C-5), 46.0 (C-18), 45.2 ($N(CH_3)_2$), 45.0 (C-19), 43.0 (C-14), 42.4 (C-8), 38.9 (C-4), 38.6 (C-1), 37.0 (C-10), 36.7 (C-16), 35.5 (C-17), 32.2 (C-7), 31.5 (C-22), 31.3 (NH*CH$_2$*), 28.6 (C-29), 28.4 (C-23), 28.2 (C-28), 27.0 (C-21), 26.1 (C-15), 25.9 (C-2), 23.1 (C-27), 18.5 (C-25), 17.3 (C-6), 16.3 (C-26), 16.1 (C-24). TOF-HRMS: *m/z* $[M + H]^+$ calcd for $C_{34}H_{58}N_3O_3$: 556.4473; found: 556.4478.

4.3.20. (S)-1-((3β,20β)-3-hydroxyl-11-oxo-olean-12-en-20-yl)-3-(propanoic acid-2-yl)urea (5r)

Method B; white powder, 59%; m.p. 226–229 °C; ^{1}H NMR (400 MHz, DMSO-d_6) δ 5.97 (d, $J = 7.8$ Hz, 1H, *NH*CH), 5.75 (s, 1H, NH), 5.46 (s, 1H, 12-H), 4.32 (brs, 1H, OH), 4.10 (dd, $J = 7.2$ Hz, 1H, NH*CH*), 3.00 (m, 1H, 3-H), 2.58 (m, 1H, 9-H), 2.31 (s, 1H, 18-H), 2.08 (m, 2H), 1.81–1.34 (m, 11*H*), 13.1 (s, 3H, 29-H), 1.17 (s, 3H, 27-H), 1.26–1.11 (m, 7H), 1.04, 1.02 (2 × s, 2 × 3H, 23-H, 24-H), 0.93 (m, 2H), 0.90 (s, 3H, 25-H), 0.79 (s, 3H, 28-H), 0.70 (m, 1H), 0.68 (s, 3H, 26-H); ^{13}C NMR (101 MHz, DMSO-d_6) δ 199.1 (C-11), 175.4 (COOH), 170.0 (C-13), 156.7 (C-30), 127.1 (C-12), 76.6 (C-3), 61.1 (C-9), 54.1 (C-20), 51.3 (C-5), 47.9 (C-18), 45.9 (C-19), 44.0 (NHCH), 42.9 (C-14), 42.2 (C-8), 38.8 (C-4), 38.5 (C-1), 36.6 (C-10), 35.3 (C-16), 32.1 (C-17), 31.2 (C-7), 31.1 (C-22), 28.4 (C-29), 28.3 (CH*CH$_3$*), 28.1 (C-28), 26.9 (C-21), 26.0 (C-15), 25.8 (C-2), 22.9 (C-27), 18.6 (C-32), 18.3 (C-25), 17.1 (C-6), 16.2 (C-26), 16.0 (C-24). TOF-HRMS: *m/z* $[M + H]^+$ calcd for $C_{33}H_{53}N_2O_5$: 557.3949; found: 557.3953.

4.3.21. (S)-1-((3β,20β)-3-hydroxyl-11-oxo-olean-12-en-20-yl)-3-(4-methylpentanoic acid-2-yl)urea (5 s)

Method B; white powder, 55%; m.p. 231–233 °C; ^{1}H NMR (400 MHz, DMSO-d_6) δ 5.93 (d, $J = 8.7$ Hz, 1H, *NH*CH), 5.70 (s, 1H, NH), 5.44 (s, 1H, 12-H), 4.31 (d, $J = 4.9$ Hz, 1H,OH), 4.11 (m, 1H, NH*CH*), 3.02 (m, 1H, 3-H), 2.58 (m, 1H, 9-H), 2.32 (s, 1H, 18-H), 2.08 (m, 2H), 1.82–1.35 (m, 14H), 1.32 (s, 3H, 29-H), 1.19 (s, 3H, 27-H),1.15 (m, 2H), 1.04, 1.02 (2 × s, 2 × 3H, 23-H, 24-H), 0.89 (m, 6H), 0.78 (s, 3H, 28-H), 0.70 (m, 1H), 0.68 (s, 3H, 26-H); ^{13}C NMR (101 MHz, DMSO-d_6) δ 199.1 (C-11), 175.4 (COOH), 170.0 (C-13), 156.8 (C-30), 127.1 (C-12), 76.6 (C-3), 61.1 (C-9), 54.1 (C-20), 51.3 (C-5), 50.4 (C-18), 46.2 (C-19), 44.8 (NCH), 43.0 (C-14), 41.6 (C-8), 38.8 (C-4), 38.5 (C-1), 36.6 (C-10), 35.2 (C-16), 32.1 (C-17), 31.6 (C-7), 31.5 (C-22), 28.4 (C-29), 28.3 (CH*CH$_2$*), 28.1 (C-28), 26.9 (C-21), 26.0 (C-15), 25.8 (C-2), 24.4 (CH*CH$_3$*), 23.0 (CH*CH$_3$*), 22.9 (C-27), 21.8 (*CH*CH$_3$), 18.4 (C-32, C-25), 17.2 (C-6), 16.2 (C-26), 16.0 (C-24). TOF-HRMS: *m/z* $[M + H]^+$ calcd for $C_{36}H_{59}N_2O_5$: 599.4400; found: 599.4403.

4.3.22. (S)-1-((3β,20β)-3-hydroxyl-11-oxo-olean-12-en-20-yl)-3-(succinic acid-2-yl)urea (5 t)

Mehtod B; white powder, 59%; m.p. 217–220 °C; ^{1}H NMR (500 MHz, DMSO-d_6) δ 6.09 (d, $J = 6.0$ Hz, 1H, *NH*CH), 6.02 (s, 1H, CONH), 5.50 (s, 1H, 12-H), 4.16 (s, 2H), 3.00 (m, 2H, 3-H), 2.54 (m, 1H, 9-H), 2.29 (s, 1H, 18-H), 2.18 (m, 1H), 2.05 (m, 2H), 1.90 (d, $J = 18.3$ Hz, 1H), 1.73–1.31 (m, 15H), 1.30 (s, 3H, 29-H), 1.18 (m, 3H), 1.14 (m, 3H), 1.02, 1.01 (2 × s, 2 × 3H, 23-H, 24-H), 0.91 (s, 2H), 0.89 (s, 3H, 25-H), 0.77 (s, 3H, 28-H), 0.68 (s, 1H), 0.67 (s, 3H, 26-H); ^{13}C NMR (126 MHz, DMSO-d_6) δ 199.4 (C-11), 174.6 (COOH), 173.4 (COOH), 170.3 (C-13), 156.9 (C-30), 127.3 (C-12), 76.8 (C-3), 61.3 (C-9), 54.2 (C-20), 51.5 (C-5), 49.5 (NCH), 45.9 (C-18), 45.0 (C-19), 43.1 (C-14), 42.5 (C-8), 38.9 (*CH$_2$*CO), 38.7 (C-4), 36.7 (C-1), 35.5 (C-10), 32.3 (C-16), 31.6 (C-17), 31.1 (C-7), 28.5 (C-22), 28.4 (C-29), 28.3 (C-23), 27.1 (C-28), 26.2 (C-21), 25.9 (C-15), 23.1 (C-2), 21.3 (C-27), 18.5 (C-25), 17.3 (C-6), 16.3 (C-26), 16.1 (C-24). TOF-HRMS: *m/z* $[M + H]^+$ calcd for $C_{34}H_{53}N_2O_7$: 601.3847; found: 601.3845.

4.3.23. (S)-1-((3β,20β)-3-hydroxyl-11-oxo-olean-12-en-20-yl)-3-(pentanedioic acid-2-yl) urea (5u)

Mehtod B; white powder, 55%; m.p. 220–222 °C; ^{1}H NMR (500 MHz,

DMSO-d_6) ^{1}H NMR (500 MHz, DMSO-d_6) δ 9.27 (s, 1H, COOH), 7.67 (s, 1H, COOH), 5.96 (s, 1H,*NH*CH), 5.86 (s, 1H, CO*NH*), 5.52 (s, 1H,12-H), 4.32 (d, J = 4.8 Hz, 1H, OH), 3.75 (dd, J = 6.1 Hz, 1H, NH*CH*), 3.02 (m, 1H, 3-H), 2.58 (m, 1H,9-H), 2.30 (s, 1H,18-H), 2.20 (m, 2H, CHCH$_2$*CH$_2$*), 2.10 (m, 2H, CH*CH$_2$*CH$_2$). 1.84–1.36 (m, 14H), 1.31 (s, 3H, 29-H), 1.19 (s, 2H), 1.13 (m, 3H), 1.03, 1.02 (2 × s, 2 × 3H, 23-H, 24-H), 0.91 (s, 2H), 0.89 (s, 3H, 25-H), 0.77 (s, 3H, 28-H), 0.68 (s, 3H, 26-H), 0.66 (s, 1H); ^{13}C NMR (126 MHz, DMSO-d_6) δ 199.2 (C-11), 176.9 (COOH), 170.2 (C-13), 157.4 (COOH), 157.0 (C-30), 127.1 (C-12), 76.6 (C-3), 61.1 (C-9), 54.1 (C-20), 51.2 (C-5), 45.7 (C-18), 44.9 (C-19), 42.9 (C-14), 42.7 (NCH), 40.5 (C-8), 38.8 (C-4), 38.6 (C-1), 36.6 (C-10), 35.4 (C-16), 32.2 (C-17), 31.4 (C-7), 31.3 (CH_2), 31.0 (C-22), 28.5 (C-29), 28.3 (C-23), 28.2 (C-28), 27.0 (C-21), 26.0 (C-15), 25.8 (C-2), 25.4 (CH_2), 23.0 (C-27), 18.4 (C-25), 17.2 (C-6), 16.2 (C-26), 16.0 (C-24). TOF-HRMS: m/z [M + H]$^+$ calcd for $C_{35}H_{55}N_2O_7$: 615.4000; found: 615.3996.

4.3.24. (S)-1-((3β,20β)-3-hydroxyl-11-oxo-olean-12-en-20-yl)-3-(5-guanidinopentanoic acid-2-yl)urea (**5v**)

Mehtod B; white powder, 52%; m.p. 220–222 °C; ^{1}H NMR (500 MHz, DMSO-d_6) δ 6.00 (d, J = 7.9 Hz, 1H, C = NH), 5.79 (s, 1H, CO*NH*), 5.50 (s, 1H, 12-H), 4.30 (brs, 1H, OH), 4.05 (m, 1H), 3.01 (m, 1H, 3-H), 2.59 (m, 1H, 9-H), 2.31 (s, 1H, 18-H), 2.27–2.07 (m, 4H), 1.94–1.35 (m, 14H), 1.32 (s, 3H, 29-H), 1.20 (m, 3H, 27-H), 1.16 (m, 2H), 1.04, 1.03 (2 × s, 2 × 3H, 23-H, 24-H), 0.94 (m, 2H), 0.91 (s, 3H, 25-H), 0.80 (s, 3H, 28-H), 0.70 (s, 1H), 0.68 (s, 3H, 26-H); ^{13}C NMR (126 MHz, DMSO-d_6) δ 199.1 (C-11), 174.6 (COOH), 173.9 (C = NH), 169.9 (C-13), 156.9 (C-30), 127.2 (C-12), 76.6 (C-3), 61.1 (C-9), 54.1 (C-20), 51.7 (NCH), 51.4 (C-5), 45.9 (C-18), 44.8 (C-19), 43.0 (NCH_2), 42.3 (C-8, C-14), 38.8 (C-4), 38.5 (C-1), 36.7 (C-10), 35.3 (C-16), 32.1 (C-17), 31.4 (C-7), 31.0 (C-22), 30.2 (CH_2), 28.32 (C-29), 28.27 (C-23), 28.1 (C-28), 28.0 (CH_2), 27.0 (C-21), 26.0 (C-15), 25.8 (C-2), 23.0 (C-27), 18.4 (C-25), 17.2 (C-6), 16.2 (C-26), 16.0 (C-24). TOF-HRMS: m/z [M + H]$^+$ calcd for $C_{36}H_{60}N_5O_5$: 642.4589; found: 642.4593.

4.4. Biological evaluation

4.4.1. Cell culture

The murine macrophage RAW 264.7 cell line obtained from BeNa Culture Collection Company. Cells were cultured in DMEM (Hyclone, USA) supplemented with 10% FBS (Biological Industries, Israel), 100 U/mL penicillin and 100 mg/mL streptomycin (Beyotime) in a humidified incubator with 5% CO_2 at 37 °C.

4.4.2. Cell viability assay

Cell viability is based on cell metabolism measured by the MTT assay. RAW264.7 cells were seeded at a density of 1 × 10^4 cells/mL in 96-well plates (three replicates) and allowed to attach overnight to become almost confluent. After adherence, the cells were treated with the same concentration of glycyrrhetic ureas (20 μM) for 12 h. Then, MTT solution (0.5 mg/mL) was added to each well for 4 h in media. The culture media were discarded and replaced with DMSO (150 μL/well) to dissolve crystals, incubated for 20 min in a constant temperature shaker, and the absorbance was read at 492 nm with a microplate reader (MQX200, Bio-Tek, USA).

4.4.3. Griess assay

NO production from activated RAW264.7 cells was determined by measuring the amount of nitrite, a relatively stable oxidation product of NO, as described previously [55]. RAW 264.7 cells were cultured in 48-well plates at a density of 7 × 10^4 cells/mL overnight. After adding different concentrations of glycyrrhetic ureas (5, 10 and 20 μM) for 1 h, cells were stimulated with LPS (500 ng/mL) for 24 h. The determination of the nitrite concentration is based on the Griess reaction by colorimetry (Griess reagent, Beyotime, China). Briefly, the Griess reagents I and II was added to 50 μL supernatant of the cultured media, and the solutions were mixed and determined at 540 nm in an automated microplate reader.

4.4.4. Measurement of inflammatory mediators

RAW264.7 cells were cultured in 48-well plates for 24 h, after glycyrrhetic ureas (5, 10 and 20 μM) were added and incubated for 1 h, then LPS solution (0.5 μg/mL) stimulated for 24 h, and the supernatant was extracted for detection. TNF-α and IL-6 release levels from macrophage supernatant were determined by ELISA kits (Huamei, Wuhan) according to manufacturers' instruction.

4.4.5. Animal experiments

Male C57BL/6 mice (6–8 weeks old, weight 18–25 g) were supplied by Animal Center of Anhui Medical University (Hefei, China). Before the experiment, all animals were allowed to feed and drink freely for 7 days at 60 ± 10% relative humidity and 23 ± 2 °C in a 12 h light/dark cycle. All animal experiments were conducted in accordance with the "Guidelines for the Care and Use of Laboratory Animals" of the National Institutes of Health. All mice were randomly divided into 3 groups (n = 10), blank control group, model group and **5r** group. Mice in **5r** group were given compound **5r** (30 mg/kg) with intragastric administration for 3 consecutive days, and the other groups were given the same amount of normal saline. On the third day, except for the normal group, all mice were injected intraperitoneally with cisplatin solution (20 mg/kg) (Aladdin, China) 1 h after intragastric administration. In the normal group, mice were injected intraperitoneally with the same dose of saline. Under the same conditions, the mice continued to be administered compound **5r** or an equal volume of saline for 3 days, and then serum and kidney tissue were obtained.

According to the manufacturer's instructions, the serum markers of renal function BUN and Scr were determined by the BUN and Scr assay kits (Nanjing Jiancheng Institute of Biotechnology, Nanjing, China). Similarly, enzyme-linked immunosorbent assay was used to detect serum levels of pro-inflammatory factors TNF-α and IL-6. The absorbance values under different wavelengths were detected using a microplate reader. Samples were taken from the kidney of mice in different groups and fixed in 10% formalin in saline for 24 h. All samples were washed in tap water for half an hour and dehydrated with ethanol. The obtained tissue sections were collected on slides, deparaffinized, and stained with hematoxylin-eosin (H&E) and periodic acid-schiff (PAS) staining for examination using a photoelectron microscope.

4.5. Statistical analysis

Unless otherwise specified, all data are expressed as the mean ± standard deviation (SD) of two or three independent experiments. The statistical significance of mean values was assessed using one-way analysis of variance (ANOVA). The SPSS 20.0 software was used to analysis the study results. A value of $p < 0.05$ indicated that the difference is statistically significant.

Declaration of Competing Interest

The authors declare that they have no known competing financial interests or personal relationships that could have appeared to influence the work reported in this paper.

Acknowledgments

Financial support was provided by Natural Science Fundation of Anhui provincial Department of Education (KJ2019ZD21), and Linyi Science and Technology Development Program (NO. 202020070).

Notes

The authors declare no competing financial interest.

Appendix A. Supplementary material

Supplementary data to this article can be found online at https://doi.org/10.1016/j.bioorg.2021.104755.

References

[1] A.S. Levey, M.T. James, Acute Kidney Injury, Ann. Intern. Med. 167 (2017). ITC66-ITC80.
[2] K. Singbartl, J.A. Kellum, AKI in the ICU: definition, epidemiology, risk stratification, and outcomes, Kidney Int. 81 (2012) 819–825.
[3] A. Zuk, J.V. Bonventre, Acute Kidney Injury, Annu. Rev. Med. 67 (2016) 293–307.
[4] C. Ronco, R. Bellomo, J.A. Kellum, Acute kidney injury, Lancet 394 (2019) 1949–1964.
[5] Y. Jiang, K.P. Rakesh, N.S. Alharbi, H.K. Vivek, H.M. Manukumar, Y.H. E. Mohammed, H.L. Qin, Radical scavenging and anti-inflammatory activities of (hetero)arylethenesulfonyl fluorides: Synthesis and structure-activity relationship (SAR) and QSAR studies, Bioorg. Chem. 89 (2019), 103015.
[6] G. Ramesh, W.B. Reeves, Inflammatory cytokines in acute renal failure, Kidney Int. Suppl. 66 (2004) S56–S61.
[7] A. Akcay, Q. Nguyen, C.L. Edelstein, Mediators of Inflammation in Acute Kidney Injury, Mediat. Inflamm. 2009 (2009), 137072.
[8] X.M. Meng, D.J. Nikolic-Paterson, H.Y. Lan, Inflammatory processes in renal fibrosis, Nat. Rev. Nephrol. 10 (2014) 493–503.
[9] S.M. Bagshaw, Short- and long-term survival after acute kidney injury, Nephrol. Dial. Transplant. 23 (2008) 2126–2128.
[10] G.M. Chertow, E. Burdick, M. Honour, J.V. Bonventre, D.W. Bates, Acute kidney injury, mortality, length of stay, and costs in hospitalized patients, J. Am. Soc. Nephrol. 16 (2005) 3365–3370.
[11] H. Rabb, M. Griffin, D. McKay, S. Swaminathan, P. Pickkers, M. Rosner, J. Kellum, C. Ronco, Inflammation in AKI: Current Understanding, Key Questions, and Knowledge Gaps, J. Am. Soc. Nephrol. 27 (2016) 371–379.
[12] C. Li, M.B. Sridhara, K.P. Rakesh, H.K. Vivek, H.M. Manukumar, C.S. Shantharam, H.L. Qin, Multi-targeted dihydrazones as potent biotherapeutics, Bioorg. Chem. 81 (2018) 389–395.
[13] S.M. Wang, G.F. Zha, K.P. Rakesh, N. Darshini, T. Shubhavathi, H.K. Vivek, N. Mallesha, H.L. Qin, Synthesis of benzo[d]thiazole-hydrazone analogues: molecular docking and SAR studies of potential H (+)/K (+) ATPase inhibitors and anti-inflammatory agents, Medchemcomm 8 (2017) 1173–1189.
[14] H.M. Revankar, S.N. Bukhari, G.B. Kumar, H.L. Qin, Coumarins scaffolds as COX inhibitors, Bioorg Chem. 71 (2017) 146–159.
[15] R. Hegazy, A. Salama, D. Mansour, A. Hassan, Renoprotective Effect of Lactoferrin against Chromium-Induced Acute Kidney Injury in Rats: Involvement of IL-18 and IGF-1 Inhibition, PLoS One 11 (2016), e0151486.
[16] M. Meissner, S. Viehmann, C. Kurts, DAMPening sterile inflammation of the kidney, Kidney Int. 95 (2019) 489–491.
[17] U. Kostakoglu, T. Mercantepe, H. Yilmaz, L. Tumkaya, S. Batcik, E. Pinarbas, H. Uydu, The Protective Effects of Perindopril Against Acute Kidney Damage Caused by Septic Shock, Inflammation (2020), https://doi.org/10.1007/s10753-020-01316-8.
[18] T. Rousselle, C. Kuscu, C. Kuscu, K. Schlegel, L. Huang, M. Namwanje, J. Eason, L. Makowski, D. Maluf, V. Mas, A. Bajwa, FTY720 Regulates Mitochondria Biogenesis in Dendritic Cells to Prevent Kidney Ischemic Reperfusion Injury, Front Immunol. 11 (2020) 1278.
[19] H. Gao, X. Wang, X. Qu, J. Zhai, L. Tao, Y. Zhang, Y. Song, W. Zhang, Omeprazole attenuates cisplatin-induced kidney injury through suppression of the TLR4/NF-κB/NLRP3 signaling pathway, Toxicology 440 (2020), 152487.
[20] W. Wu, J. Wang, Z. Li, B. Wei, J. Jin, L. Gao, H. Li, J. Li, H. Chen, X. Meng, 7-Hydroxycoumarin protects against cisplatin-induced acute kidney injury by inhibiting necroptosis and promoting Sox9-mediated tubular epithelial cell proliferation, Phytomedicine 69 (2020), 153202.
[21] X. Liu, J. Jin, Z. Li, L. Jiang, Y. Dong, Y. Cai, M. Wu, J. Wang, T. Ma, J. Wen, M. Liu, J. Li, Y. Wu, X. Meng, Rutaecarpine derivative Cpd-6c alleviates acute kidney injury by targeting PDE4B, a key enzyme mediating inflammation in cisplatin nephropathy, Biochem. Pharmacol. 180 (2020), 114132.
[22] M.N. Asl, H. Hosseinzadeh, Review of pharmacological effects of *Glycyrrhiza* sp. and its bioactive compounds, Phytother. Res. 22 (2008) 709–724.
[23] W.J. Tang, Y.A. Yang, H. Xu, J.B. Shi, X.H. Liu, Synthesis and discovery of18α-GAMG as anticancer agent *in vitro* and *in vivo via* down expression of protein p65, Sci. Rep. 4 (2014) 7106.
[24] M.N. Oztanir, O. Ciftci, A. Cetin, M.A. Durak, N. Basak, Y. Akyuva, The beneficial effects of 18β-glycyrrhetic acid following oxidative and neuronal damage in brain tissue caused by global cerebral ischemia/reperfusion in a C57BL/J6 mouse model, Neurol. Sci. 35 (2014) 1221–1228.
[25] B. Li, Y. Yang, L. Chen, S. Chen, J. Zhang, W. Tang, 18alpha-Glycyrrhetinic acid monoglucuronide as an anti-inflammatory agent through suppression of the NF-kappaB and MAPK signaling pathway, Medchemcomm 8 (2017) 1498–1504.
[26] C. Wu, A. Chen, G. Yen, Protective Effects of Glycyrrhizic Acid and 18β-Glycyrrhetinic Acid against Cisplatin-Induced Nephrotoxicity in BALB/c Mice, J. Agric. Food Chem. 63 (2015) 1200–1209.
[27] S. Abd El-Twab, W. Hozayen, O. Hussein, A. Mahmoud, 18β-Glycyrrhetinic acid protects against methotrexate-induced kidney injury by up-regulating the Nrf2/ARE/HO-1 pathway and endogenous antioxidants, Ren. Fail. 38 (2016) 1516–1527.
[28] X. Cheng, L. Qiu, F. Wang, 18α-Glycyrrhetinic acid (GA) ameliorates fructose-induced nephropathy in mice by suppressing oxidative stress, dyslipidemia and inflammation, Biomed. Pharmacother. 125 (2020), 109702.
[29] Z. Guo, The modification of natural products for medical use, Acta Pharm. Sin. B. 7 (2017) 119–136.
[30] S. Wang, G. Dong, C. Sheng, Structural simplification of natural products, Chem. Rev. 119 (2019) 4180–4220.
[31] H.L. Qin, Z.W. Zhang, L. Ravindar, K.P. Rakesh, Antibacterial activities with the structure-activity relationship of coumarin derivatives, Eur J Med Chem. 207 (2020), 112832.
[32] R. Csuk, S. Schwarz, B. Siewert, R. Kluge, D. Ströhl, Conversions at C-30 of glycyrrhetinic acid and their impact on antitumor activity, Archiv. der Pharmazie. 345 (2012) 223–230.
[33] B. Li, S. Cai, Y.A. Yang, S.C. Chen, R. Chen, J.B. Shi, X.H. Liu, W.J. Tang, Novel unsaturated glycyrrhetic acids derivatives: Design, synthesis and anti-inflammatory activity, Eur. J. Med. Chem. 139 (2017) 337–348.
[34] D. Alho, J. Salvador, M. Cascante, S. Marin, Synthesis and Antiproliferative Activity of Novel A-Ring Cleaved Glycyrrhetinic Acid Derivatives, Molecules 24 (2019) 2938.
[35] J. Sun, H. Liu, C. Lv, J. Qin, Y. Wu, Modification, Antitumor Activity, and Targeted PPARγ Study of 18β-Glycyrrhetinic Acid, an Important Active Ingredient of Licorice, J. Agric. Food Chem. 67 (2019) 9643–9651.
[36] S. Liang, M. Li, X. Yu, H. Jin, Y. Zhang, L. Zhang, D. Zhou, S. Xiao, Synthesis and structure-activity relationship studies of water-soluble β-cyclodextrin-glycyrrhetinic acid conjugates as potential anti-influenza virus agents, Eur. J. Med. Chem. 166 (2019) 328–338.
[37] Y. Yang, Q. Zhu, Y. Zhong, X. Cui, Z. Jiang, P. Wu, X. Zheng, K. Zhang, S. Zhao, Synthesis, anti-microbial and anti-inflammatory activities of 18β-glycyrrhetinic acid derivatives, Bioorg. Chem. 101 (2020), 103985.
[38] X. Chen, J. Leng, K.P. Rakesh, N. Darshini, T. Shubhavathi, H.K. Vivek, et al., Synthesis and molecular docking studies of xanthone attached amino acids as potential antimicrobial and anti-inflammatory agents, Medchemcomm. 8 (8) (2017) 1706–1719.
[39] R. Csuk, S. Schwarz, B. Siewert, R. Kluge, D. Strohl, Synthesis and antitumor activity of ring A modified glycyrrhetic acid derivatives, Eur. J. Med. Chem. 46 (2011) 5356–5369.
[40] J. Regan, S. Breitfelder, P. Cirillo, T. Gilmore, A. Graham, E. Hickey, B. Klaus, J. Madwed, M. Moriak, N. Moss, C. Pargellis, S. Pav, A. Proto, A. Swinamer, L. Tong, C. Torcellini, Pyrazole urea-based inhibitors of p38 MAP kinase: from lead compound to clinical candidate, J. Med. Chem. 45 (2002) 2994–3008.
[41] A. Jagtap, N. Kondekar, A. Sadani, J. Chern, Ureas: Applications in Drug Design, Curr. Med. Chem. 24 (2017) 622–651.
[42] S. Codony, E. Pujol, J. Pizarro, F. Feixas, E. Valverde, M.I. Loza, J.M. Brea, E. Saez, J. Oyarzabal, A. Pineda-Lucena, B. Perez, C. Perez, M.I. Rodriguez-Franco, R. Leiva, S. Osuna, C. Morisseau, B.D. Hammock, M. Vazquez-Carrera, S. Vazquez, 2-Oxaadamant-1-yl Ureas as Soluble Epoxide Hydrolase Inhibitors. In Vivo Evaluation in a Murine Model of Acute Pancreatitis, J. Med. Chem. 63 (2020) 9237–9257.
[43] K. Okamoto, M. Ikemori-Kawada, A. Jestel, K. von König, Y. Funahashi, T. Matsushima, A. Tsuruoka, A. Inoue, J. Matsui, Distinct binding mode of multikinase inhibitor lenvatinib revealed by biochemical characterization, ACS Med. Chem. Lett. 6 (2015) 89–94.
[44] C. Bogdan, Nitric oxide and the immune response, Nat. Immunol. 2 (2001) 907–916.
[45] D.M. Mosser, J.P. Edwards, Exploring the full spectrum of macrophage activation, Nat. Rev. Immunol. 8 (2008) 958–969.
[46] M. Rossol, H. Heine, U. Meusch, D. Quandt, C. Klein, M.J. Sweet, S. Hauschildt, LPS-induced Cytokine Production in Human Monocytes and Macrophages, Crit. Rev. Immunol. 31 (2011) 379–446.
[47] J.S. Deng, W.P. Jiang, C.C. Chen, L.Y. Lee, P.Y. Li, W.C. Huang, J.C. Liao, H. Y. Chen, S.S. Huang, G.J. Huang, Cordyceps cicadae Mycelia Ameliorate Cisplatin-Induced Acute Kidney Injury by Suppressing the TLR4/NF-kappaB/MAPK and Activating the HO-1/Nrf2 and Sirt-1/AMPK Pathways in Mice, Oxid. Med. Cell Longev. 2020 (2020) 7912763.
[48] L. Patzer, Nephrotoxicity as a cause of acute kidney injury in children, Pediatr. Nephrol. 23 (2008) 2159–2173.
[49] G.S. Oh, H.J. Kim, A. Shen, S.B. Lee, D. Khadka, A. Pandit. S. HS, Cisplatin-induced Kidney Dysfunction and Perspectives on Improving Treatment Strategies, Electrolyte Blood Press 12 (2014) 55-65.
[50] D. Moledina, C. Parikh, Phenotyping of Acute Kidney Injury: Beyond Serum Creatinine, Semin. Nephrol. 38 (2018) 3–11.
[51] Z. Qi, W. Li, J. Tan, C. Wang, H. Lin, B. Zhou, J. Liu, P. Li, Effect of ginsenoside Rh on renal apoptosis in cisplatin-induced nephrotoxicity in vivo, Phytomedicine 61 (2019), 152862.
[52] I. Rjeibi, A. Feriani, A. Ben Saad, J. Sdayria, I. Saidi, S. Ncib, S. Souid, M. Allagui, N. Hfaiedh, Lycium europaeum Extract: A New Potential Antioxidant Source against Cisplatin-Induced Liver and Kidney Injuries in Mice, Oxid. Med. Cell Longev. (2018, 2018,) 1630751.

[53] L.S. Chawla, P.L. Kimmel, Acute kidney injury and chronic kidney disease: an integrated clinical syndrome, Kidney Int. 82 (2012) 516–524.
[54] D. Martin-Sanchez, O. Ruiz-Andres, J. Poveda, S. Carrasco, P. Cannata-Ortiz, M. D. Sanchez-Nino, M. Ruiz Ortega, J. Egido, A. Linkermann, A. Ortiz, A.B. Sanz, Ferroptosis, but Not Necroptosis, Is Important in Nephrotoxic Folic Acid-Induced AKI, J. Am. Soc. Nephrol. 28 (2017) 218–229.
[55] L. Chen, L. Yao, M. Jiao, J. Shi, Y. Tan, B. Ruan, X. Liu, Novel resveratrol-based flavonol derivatives: Synthesis and anti-inflammatory activity *in vitro* and *in vivo*, Eur. J. Med. Chem. 175 (2019) 114–128.